



# Intrinsic properties of Boolean dynamics in complex networks

Shu-ichi Kinoshita<sup>a,\*</sup>, Kazumoto Iguchi<sup>b</sup>, Hiroaki S. Yamada<sup>c</sup>

<sup>a</sup> Graduate School of Science and Technology, Niigata University, Nishi-ku Ikarashi 2-Nochou 8050, Niigata 950-2181, Japan

<sup>b</sup> Kazumotolguchi Research Laboratory, 70-3 Shinhari, Hari, Anan, Tokushima 774-0003, Japan

<sup>c</sup> Yamada Physics Research Laboratory, Nishi-ku Aoyama 5-7-14, Niigata 950-2002, Japan

## ARTICLE INFO

### Article history:

Received 19 April 2008

Received in revised form

14 October 2008

Accepted 14 October 2008

Available online 29 October 2008

### Keywords:

Boolean dynamics

Attractor

Scale-free network

Intrinsic property

Robustness

Frozen nodes

## ABSTRACT

We study intrinsic properties of attractor in Boolean dynamics of complex networks with scale-free topology, comparing with those of the so-called Kauffman's random Boolean networks. We numerically study both frozen and relevant nodes in each attractor in the dynamics of relatively small networks ( $20 \leq N \leq 200$ ). We investigate numerically robustness of an attractor to a perturbation. An attractor with cycle length of  $\ell_c$  in a network of size  $N$  consists of  $\ell_c$  states in the state space of  $2^N$  states; each attractor has the arrangement of  $N$  nodes, where the cycle of attractor sweeps  $\ell_c$  states. We define a perturbation as a flip of the state on a single node in the attractor state at a given time step. We show that the rate between unfrozen and relevant nodes in the dynamics of a complex network with scale-free topology is larger than that in Kauffman's random Boolean network model. Furthermore, we find that in a complex scale-free network with fluctuation of the in-degree number, attractors are more sensitive to a state flip for a highly connected node (i.e. input-hub node) than to that for a less connected node. By some numerical examples, we show that the number of relevant nodes increases, when an input-hub node is coincident with and/or connected with an output-hub node (i.e. a node with large output-degree) one another.

© 2008 Elsevier Ltd. All rights reserved.

## 1. Introduction

One of the most remarkable features in “life” or a “living system” is coexistence between evolvability and robustness. Diversity of cell type in organism is such a typical example. Indeed, an embryo-stem (ES) cell differentiates into various types of cells with different phenotypes, depending on multiple environmental factors; the cell can repeat stably cell division. It can be regarded as an irreversible transition in evolution as pointed out by Maynard Smith and Szathmary (1995, 1999). The process of cell differentiation obeys dynamical rules of gene–gene interactions. Recent genome sequencing and gene expression profiling projects have produced a huge amount of experimental data to investigate evolutionary processes such as robustness and evolvability (Kohane et al., 2002; Shen-Orr et al., 2002; Ueda et al., 2004).

Kauffman (1969) introduced the so-called *Kauffman model*—random Boolean network (RBN) model, based upon random network theory as a simplified model for a complex interaction in gene regulatory networks (GRNs) of living cells (Kauffman, 1993, 2004a; Sawhill and Kauffman, 1997). The network in the

model consists of  $N$  nodes, each of which receives inputs from  $K$  other nodes randomly chosen. The state of a node is synchronously updated in time step, following the rule of a Boolean function assigned on each node such that a collection of all states for the  $N$  nodes represents a state for the entire system of the network. Eventually, a trajectory starting from any initial state runs into an attractor (i.e. a point or a cycle), where trajectory means an orbit that a state moves in state space. A cyclic attractor is periodically repeating succession of the state. All trajectories that converge into a same attractor construct a basin of attraction. The Kauffman model has been applied to a lot of research fields in physics (Rohlf et al., 2007), biology, computational science and social science (Paczuski et al., 2000). In particular, it has been extensively applied to metabolic networks, autocatalytic networks and protein interaction networks in biological fields (Kauffman, 2004b; Li et al., 2004).

RBNs are networks with homogeneous topology, where all nodes keep an identical number of inputs. However, in a real system, each node has its own number of inputs different from one another. As a more realistic modeling of biological systems, we expect that fluctuation of the number of input-degrees is treated as a random variable with a probability distribution function such as an inverse power-law or an exponential or a Poisson distribution. In fact, the in-degree distribution  $P(k)$  is an exponential one in *Escherichia coli* and a power-law of  $P(k) \propto k^{-\gamma}$  in yeast (Barabási et al., 1999; Barabási and Oltvai, 2004; Lee et al.,

\* Corresponding author. Tel./fax: +81 252 282 948.

E-mail addresses: [f01j006g@mail.cc.niigata-u.ac.jp](mailto:f01j006g@mail.cc.niigata-u.ac.jp) (S.-i. Kinoshita), [hyamada@uranus.dti.ne.jp](mailto:hyamada@uranus.dti.ne.jp) (H.S. Yamada).

2002; Sen et al., 2003; Kauffman et al., 2003; Skarja et al., 2004; Albert, 2006). It is well known that scale-free topology is ubiquitous in nature and the degree exponent  $\gamma$  lies in between 2 and 3. Study on Boolean dynamics in the Kauffman model with a directed scale-free network (SFRBN) has started around about 2000 (Kauffman, 2004a; Albert and Barabási, 2000, 2002; Oosawa and Savageau, 2002; Wang and Chen, 2002; Aldana, 2003; Castro e Silva et al., 2004; Iguchi et al., 2005; Kauffman, 2003).

A biological system such as a GRN is robust against an internal or an external noise such as a gene mutation or an environmental perturbation (Wagner, 2005). Robustness must be consistent with evolvability in a biological system (Aldana et al., 2007; Braunewell and Bornholdt, 2007; Szejka and Drossel, 2007; Ciliberti et al., 2007). Some topological features of a regulatory network help to give the system attack tolerance. In nature, a complex network structure with such intrinsic topological properties is established as a result of evolution of the biological system. Robustness against the genetic mutation and the environmental perturbation is one of the universal features of biological systems. It is important to understand evolutionary processes and the origin of cellular complexity (Bar-Yam and Epstein, 2004; Monte et al., 2005; Liu and Bassler, 2006; Wang et al., 2007; Krawitz and Shmulevich, 2007a). Indeed, GRN exhibits homeostasis. Aldana et al. investigated small SFRBN of  $N = 15–19$  and found that robustness of an ordered phase against an external noise is lower

**Table 1**  
Definitions for node types.

Type of node	Definition
Frozen node in an attractor	Node whose state remains constant through a given trajectory of an attractor
Frozen node in a network	Node that is frozen for all attractors in Boolean dynamics on a network
Unfrozen node in an attractor	Node whose state changes through a given trajectory of an attractor
Unfrozen node in a network	Node that is unfrozen for all attractors in Boolean dynamics on a network
Relevant node in a network	Unfrozen node that constitutes a directed loop of directed links and that makes a relevant loop in a network
Irrelevant node in a network	Node that is not frozen but slaved by a relevant node

than that in RBN. The result implies that there exists a possibility that evolution occurs through mutation even in ordered phase, which is in contrast with Kauffman's conjecture that life evolves in the "edge of chaos".

The relationship between stability of network structure and robustness of attractors to perturbation is very important to understand a realistic GRN (Oikonomou and Cluzel, 2006; Gardenes et al., 2006). Stability and robustness must be mutually correlated with each other. For example, Bornholdt and Sneppen

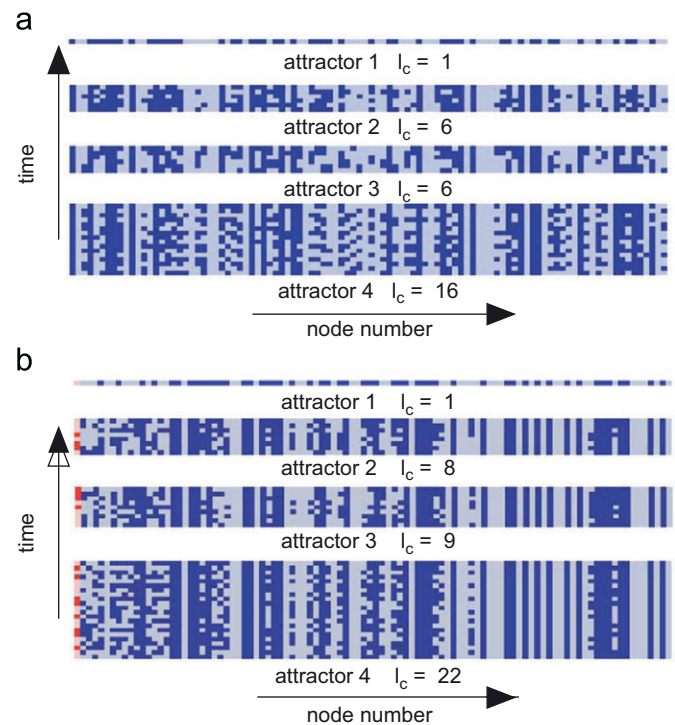


**Fig. 2.** (Color online) Temporal behaviors of attractors in (a) RBN with  $K = 2$  (b) SFRBN with  $\langle k \rangle = 2$ , where  $N = 100$ . The vertical axis denotes the temporal change, while the horizontal axis denotes the node number in the high connectivity order. The dense or gray color corresponds to binary values of the state. The point attractors consist of the only gray or dense color.

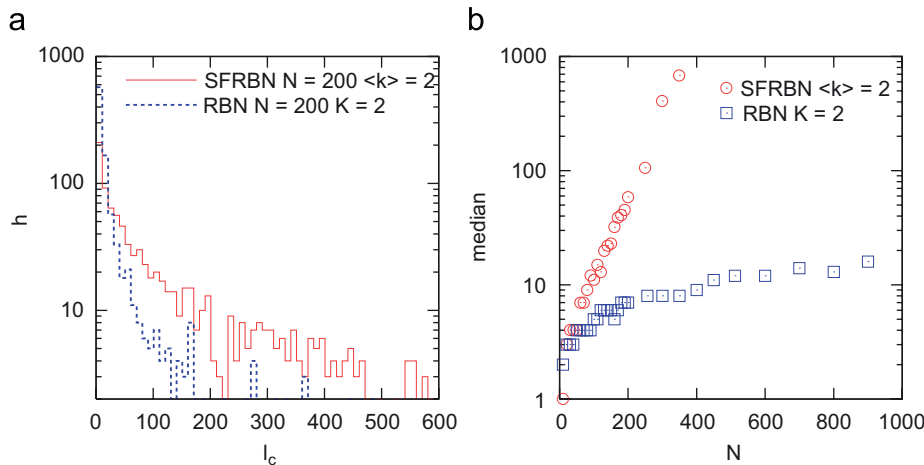


**Fig. 1.** (Color online) (a) Histogram of the length  $\ell_c$  of state cycles is shown for RBN with  $K = 2$  and SFRBN with  $\langle k \rangle = 2$ , respectively, where the network size is  $N = 200$ . The histogram is generated by 1000 different sets of the Boolean functions and five different network structures. The maximum iteration number of the Boolean dynamics is  $10^5$  until the convergence to the cycle is realized. (b) Semi-log plots of the median  $\bar{m}$  of 1000 samples of the lengths of the state cycles with respect to the total number  $N$  of nodes for the directed RBN with  $K = 2$  and the directed SFRBN with  $\langle k \rangle = 2$ .

(2000) have proposed a model that network linking is self-organized by cooperating with giving robustness against dynamical patterns. However, in this paper we are going to study a sufficiently simple model so that we can simulate the Boolean dynamics in a fixed network structure without influencing the network growth itself.

In the paper of Iguchi et al. (2007) interdependence between dynamics and topology of the network has been investigated. They found a qualitative transition in a function form of median value  $\bar{m}$  over a distribution of attractor lengths as a function of finite  $N$ , changing the average degree  $\langle k \rangle$ . Function form  $\bar{m}(N)$  asymptotically changes from an algebraic type  $\bar{m}(N) \propto N^2$  to an exponential one as the average degree  $\langle k \rangle$  goes to  $\langle k \rangle = 2$ . This is consistent with the transition that occurs at the critical value of the degree of nodes ( $K_c = 2$ ) in RBN (Kauffman, 2003; Bastolla and Parisi, 1997; Aldana et al., 2003; Socolar and Kauffman, 2003).

Hence, we are led to a question: *How does the characteristics of the attractor depend on the network topology?* In a short report (Kinoshita et al., 2008a, b), we have partially given a preliminary result for frozen nodes and robustness of attractor for SFRBN with  $\langle k \rangle = 2$ . In this paper, focusing on frozen nodes and robustness against the external perturbation we will intensively study the difference between attractors in RBN and those in SFRBN without a bias for Boolean functions. In Boolean dynamics on a complex network with a fluctuation of the number of input-degrees, we will investigate how intrinsic the property of the attractor state is, comparing with a random Kauffman network with an identical mean connectivity  $\langle k \rangle = K$ .

First, we investigate the so-called *frozen nodes* in an attractor, the number of which remains constant through a given trajectory, comparing RBN with SFRBN (Kauffman, 1993; Liu and Bassler, 2006). Definitions for node types that we use in this paper are summarized as Table 1. Frozen nodes emerge from canalization of Boolean functions and homogeneity bias as consequence of a kind of the forcing structure (Kauffman, 1993; Liu and Bassler, 2006). The shape of distribution function for the number of frozen nodes in SFRBN with  $\langle k \rangle = 2$  shows a quite different structure from that in RBN with  $K = 2$ . The peak moves to the one around the origin when connectivity of the system is increasing. The difference in the shape of distribution functions between SFRBN and RBN disappears in cases with  $\langle k \rangle = K = 4$ . Furthermore, we investigate network structures that consist of only unfrozen nodes. We find different properties between SFRBN with  $\langle k \rangle = 2$  and RBN with  $K = 2$ . Generally speaking, the number of relevant nodes in SFRBN with  $\langle k \rangle = 2$  is larger than that in RBN with  $K = 2$ .

Second, we mainly investigate the probability that a perturbed state remains in an original attractor after inversion of a single node (or multi-nodes) in the state. In general, an attractor is sensitive to perturbation to a relevant node. Accordingly, there exist many more sensitive nodes in SFRBN with  $\langle k \rangle = 2$  than in RBN with  $K = 2$  (Bilke and Sjunnesson, 2001). Furthermore, we find that as the average in-degree  $\langle k \rangle$  is increased, robustness against perturbation is enhanced. The difference between SFRBN with  $\langle k \rangle = 2$  and RBN with  $K = 2$  appears in entropy through transition probability between attractors. We find that attractors in complex networks with scale-free topology of  $\langle k \rangle = 3$  and 4 are more robust against a state flip than those in random Kauffman networks.

The organization of the paper is the following: in Section 2, we present some basic properties of RBN and SFRBN. In Section 3, we study frozen nodes in an attractor in RBN and SFRBN. In Section 4, we study the robustness of attractors to the external perturbation for various network systems. In Section 5 we discuss the relationship between frozen nodes and robustness against perturbation, based on numerical examples. In Section 6 summary and discussion are given.

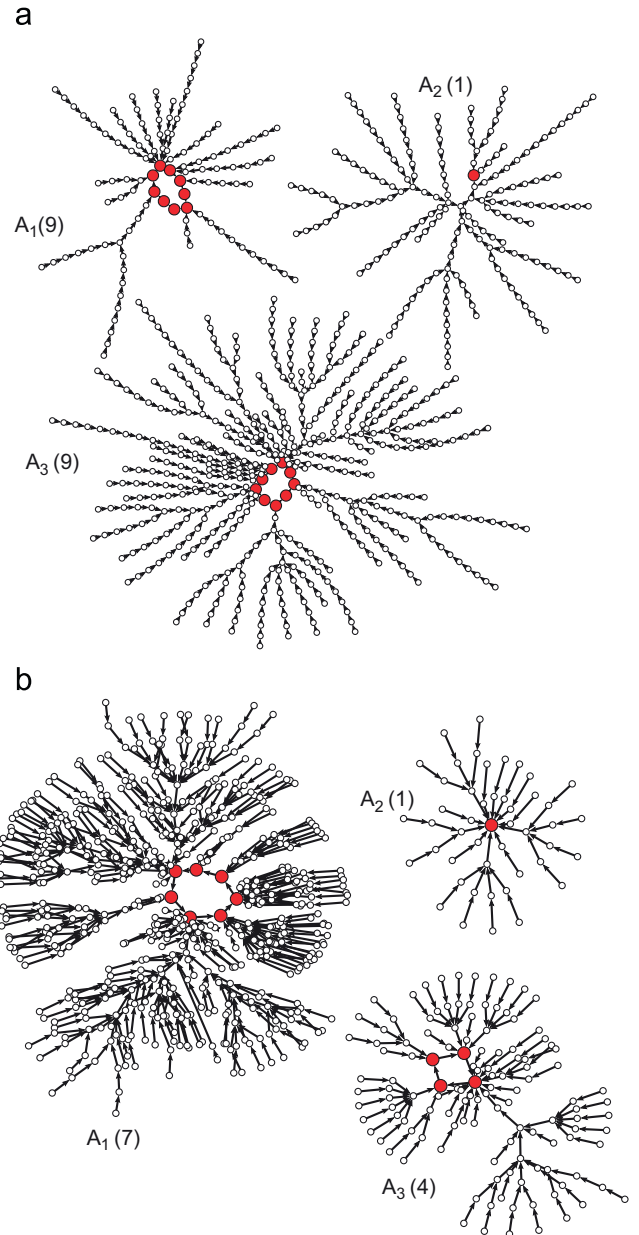


**Fig. 3.** (Color online) Some periodic attractors ( $A_i, i = 1, \dots, N_A$ ) and basins of attraction in typical (a) RBN with  $K = 2$  and (b) SFRBN with  $\langle k \rangle = 2$ , respectively. Here  $N = 40$  has been adopted. Each point in state space represents a state of the entire network (i.e. network state). An arrow indicates direction of the dynamical flow. Filled circles denote attractor states. The number of attractors is  $N_A = 3$  for RBN with  $K = 2$  and  $N_A = 3$  for SFRBN with  $\langle k \rangle = 2$ , respectively. The number in bracket of attractor symbol  $A_i$  denotes the period of the attractor.

## 2. Boolean network models and preliminary considerations

Let us consider a network that consists of  $N$  nodes and  $\{k_i\}$  links are assigned for each node  $i$ . We define a binary state  $\sigma_i \in \{0, 1\}$  on each node such that a state of the whole network can be represented by  $\{\sigma_1, \dots, \sigma_i, \dots, \sigma_N\}$ . The value of  $\sigma_i$  is determined by the following dynamical evolution equation:

$$\sigma_i(t+1) = f_i(\sigma_{i_1}(t), \sigma_{i_2}(t), \dots, \sigma_{i_{k_i}}(t)), \quad (1)$$

where  $f_i$  is a Boolean function assigned for the  $i$ th node, and it is randomly chosen from  $2^{2^{k_i}}$  Boolean functions. The initial values for the nodes are chosen randomly and states for the nodes are synchronously updated in the course of time step, according to

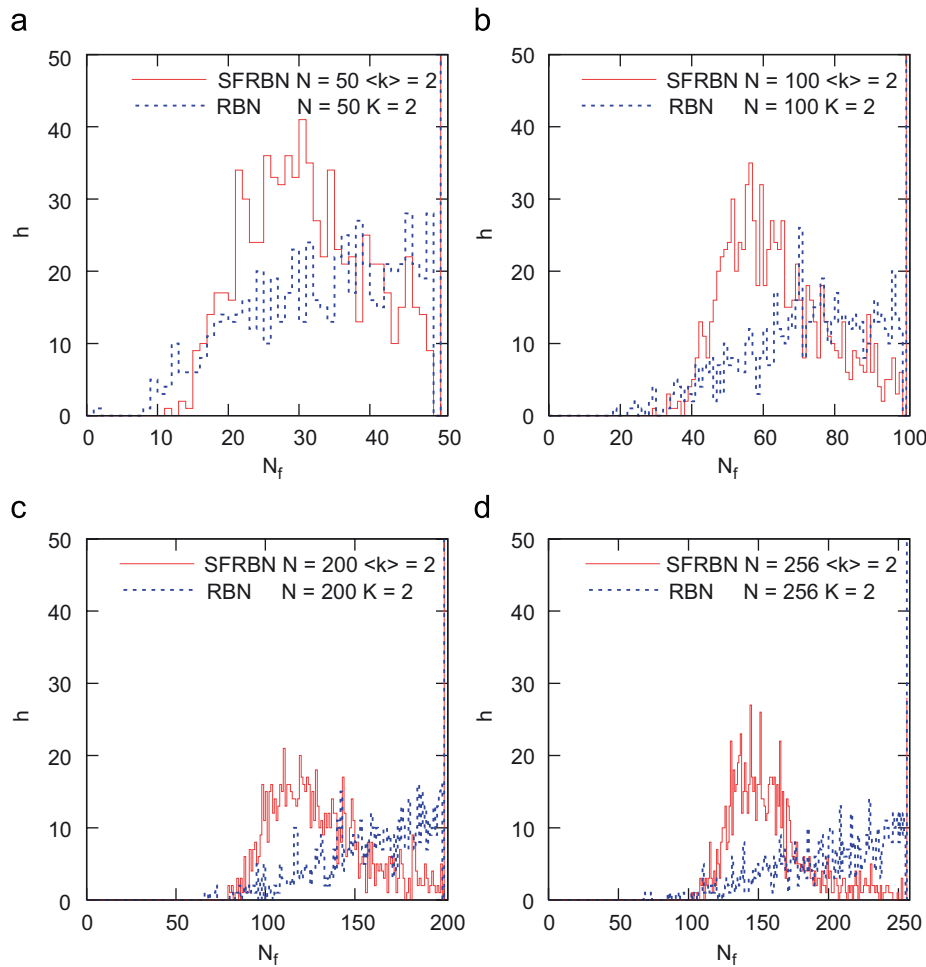


**Fig. 4.** (Color online) Histogram for the number  $N_f$  of frozen nodes for each attractor, where we consider 1000 different attractors in RBN with  $K = 2$  and SFRBN with  $\langle k \rangle = 2$ . Network size is (a)  $N = 50$ , (b)  $N = 100$ , (c)  $N = 200$ , and (d)  $N = 256$ . The scale out data at  $N_f = N$  are not shown in the figures. The 1000 different attractors are taken for 1000 different network structures with the same initial state.

connectivity  $\{k_i\}$  and Boolean functions  $\{f_i\}$  of the network. In the present paper, the number of in-degree  $k_i$  at the  $i$ th node is determined by a preferential attachment rule that makes the system a complex network with scale-free topology (Albert and Barabási, 2000). We deal with not large networks but relatively small networks (i.e.  $20 \leq N \leq 200$ ), focusing on intrinsic properties of Boolean dynamics on a complex network. We give a brief explanation for the method for generating a network in Appendix A. A full detail of the method for generating a network has been given by Iguchi et al. (2007).

As is numerically seen in relatively small networks, we would like to note that, the degree distribution function  $P(k)$  is not so definite even if the network shows a different topology for a large size of  $N$ . However, we would like to mention that network size in our study is larger than that adapted in related studies previously studied by other researchers (Oosawa and Savageau, 2002; Aldana, 2003; Aldana et al., 2007; Iguchi et al., 2007; Fox and Hill, 2001; Serra et al., 2003; Aldana and Cluzel, 2003; Handrey et al., 2007), and that our study provides a more detail of robustness of an attractor and frozen nodes in an attractor. Note that the distribution of attractors is strongly influenced by whether the adjacency matrix is symmetric or antisymmetric. Throughout this paper, we study an irreducible directed RBN and an irreducible directed SFRBN without a special symmetry.

Fig. 1(a) shows histogram of the number of attractors as a function of cycle length  $\ell_c$  of attractor in the RBN with  $K = 2$  and

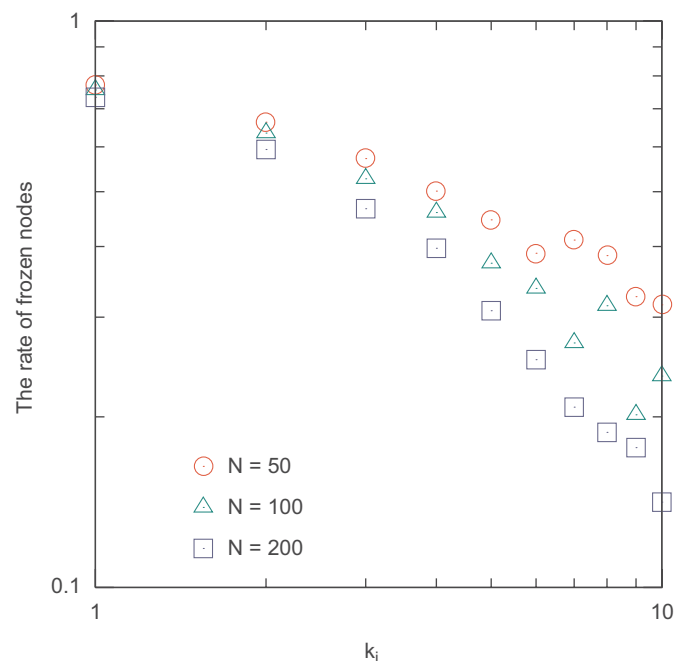


**Fig. 5.** (Color online) The rate of frozen nodes is shown as a function of connectivity in SFRBN with  $\langle k \rangle = 2$  for some network sizes ( $N = 50, 100, 200$ ).

in SFRBN with  $\langle k \rangle = 2$ , where the average degree of node  $\langle k \rangle$  is given by  $\langle k \rangle = 2$ .

Fig. 1(b) shows median value  $\bar{m}$  for the distribution of state cycle lengths with respect to the total number of nodes  $N$ . Apparently, the distribution of attractor lengths in SFRBN is much wider than that in RBN so that attractor lengths of most attractors in SFRBN have longer periods than those in RBN. This is directly related to the diversity of attractors in SFRBN, which is of great importance for the stability of a living cell.

As mentioned in the Introduction, the asymptotic change of  $\bar{m}(N)$  has been studied in detail in the paper of Iguchi et al. (2007). However, without touching the point, we mainly investigate the difference in intrinsic properties between attractors in RBN and those in SFRBN in the following sections.

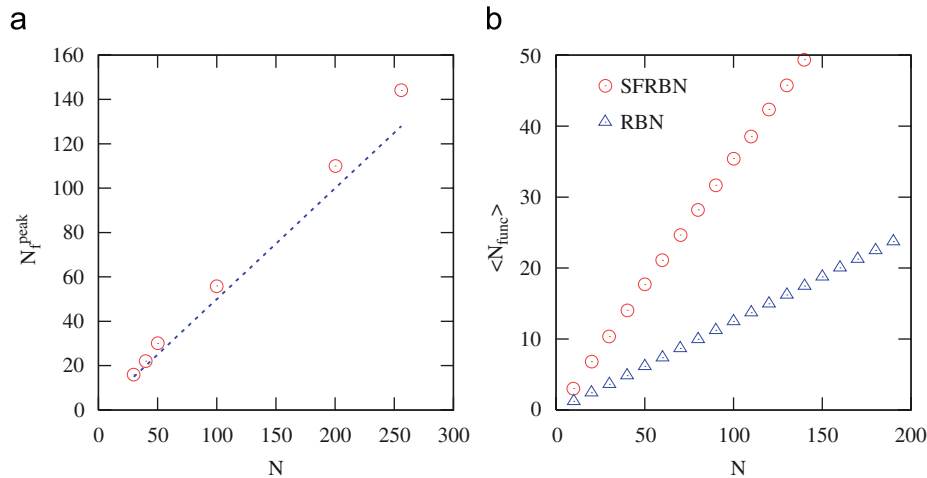
Before closing this section, in Fig. 2 we briefly show typical temporal behaviors of an attractor in an SFRBN with  $\langle k \rangle = 2$ . There is a tendency that frozen nodes in the network are almost fixed, irrespective of class of the attractor in the cases. A full detail of frozen nodes is investigated in the next section.

Fig. 3 shows some typical patterns of attractors and transient states in a typical RBN with  $K = 2$  and a typical SFRBN with

$\langle k \rangle = 2$ , respectively, where  $N = 40$  is taken. Any state in state space enters into a periodic attractor such as the one with cycle length  $\ell_c$  through transient state, starting from an initial state. Not every state of the network is a part of a periodic attractor; other states lie in transition states that do not lie in the attractor. The set of an attractor and its transition states forms a basin of attraction. Due to the deterministic dynamics, none of the basins of attraction can overlap with each other, so that the state space is divided into a number of periodic attractors according to basins of attraction. We find that transient states for SFRBN with  $\langle k \rangle = 2$  is more complex than those for RBN with  $K = 2$ . In general, the number of attractors in SFRBN is larger than that in RBN. From this situation, it is much harder to perform numerical calculations for attractor states in a large network size of SFRBN than to do those in a large network size of RBN.

### 3. Frozen nodes and relevant nodes

In this section, we are going to investigate frozen nodes in an attractor whose value remains constant through a given trajectory



**Fig. 6.** (Color online) (a) The peak position  $N_f^{peak}$  is shown as a function of network size  $N$  in histogram of the number of frozen nodes in SFRBN with  $\langle k \rangle = 2$ . The straight line of slope  $\frac{1}{2}$  is drawn as a guide for eyes. (b) The average number  $\langle N_{func} \rangle$  of frozen functions assigned to the node is shown as a function of the network size. The average is taken over 1000 different network samples.

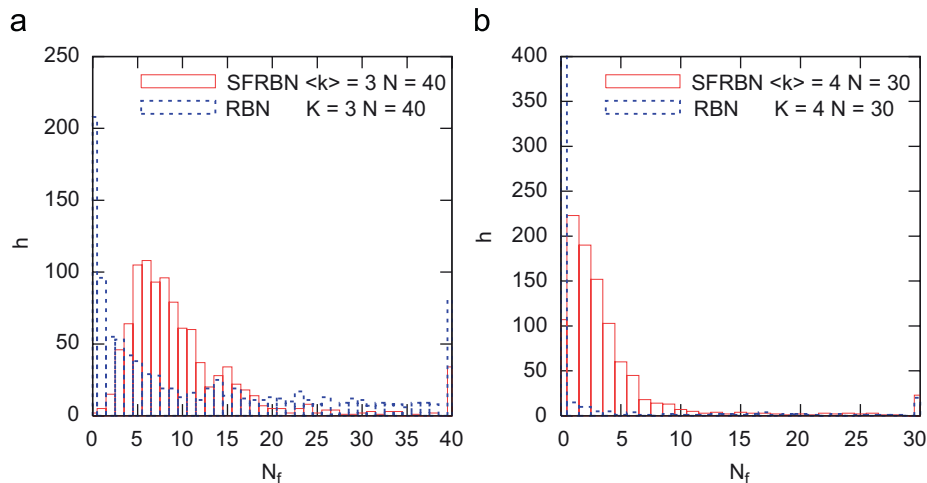


**Fig. 7.** (Color online) (a) Histogram for the number of frozen nodes  $N_f$  for each attractor, where we consider 100 attractors in both RBN with  $K = 3$  and SFRBN with  $\langle k \rangle = 3$  and  $N = 40$ . (b) Histogram of the number of frozen nodes  $N_f$  for each attractor, where we consider 100 attractors in both RBN with  $K = 4$  and SFRBN with  $\langle k \rangle = 4$  and  $N = 30$ . The 100 different attractors are taken for 100 different network structures with the same initial state.

of the attractor (Kauffman, 1993; Aldana et al., 2003). A Boolean function is canalizing if at least one of its inputs is able to determine the function's output, regardless of values of any other inputs to the node. Canalization produces robustness of the network against random perturbation since it suppresses the change of output (Justa et al., 2004). Accordingly, the number of frozen nodes increases as the rate of canalizing functions in a Boolean network is increasing. Indeed, it is known that real GRNs have many canalizing functions including frozen functions. Frozen nodes appear as a result of canalization of Boolean functions and homogeneity bias (Greil and Drossel, 2007; Drossel, 2008).

### 3.1. The number of frozen nodes in a network

Each attractor has frozen nodes whose states remain constant through time evolution. Here we call frozen nodes for all attractors in a network “frozen nodes in a network” and call other nodes “unfrozen nodes in a network”. The definitions for node types are summarized in Table 1.

We count the number of frozen nodes  $N_f$  for each attractor and plot a histogram for several cases in Fig. 4. In all the cases there are sharp peaks at  $N_f = N$ . Note that the peak at  $N_f = N$  corresponds to point attractors that all nodes in the network are frozen.

We see a remarkably different peak structure between the case in SFRBN with  $\langle k \rangle = 2$  and the case in RBN with  $K = 2$ . The distribution for SFRBN has a peak around  $N_f \approx N/2 - 2N/3$ , while the distribution for RBN is broad with a different peak at  $N_f = N$ . We show that such remarkably different characteristics between distributions of frozen nodes for RBN and SFRBN become clear more and more, as network size  $N$  increases.

We next investigate how frozen nodes are distributed in a network, where the network has an in-degree (i.e. connectivity or link) distribution of  $P(k)$ . A frozen node emerges on a node of in-degree  $k_i$  in the network. Since the in-degree distribution defines the number (or fraction) of nodes of  $k_i$  in the network, a number of nodes in the nodes of  $k_i$  become frozen nodes. Thus, we can define the rate  $R_f(k_i)$  of frozen nodes in the nodes of  $k_i$  as a ratio between frozen and unfrozen nodes in the set of all nodes of in-degree  $k_i$ .

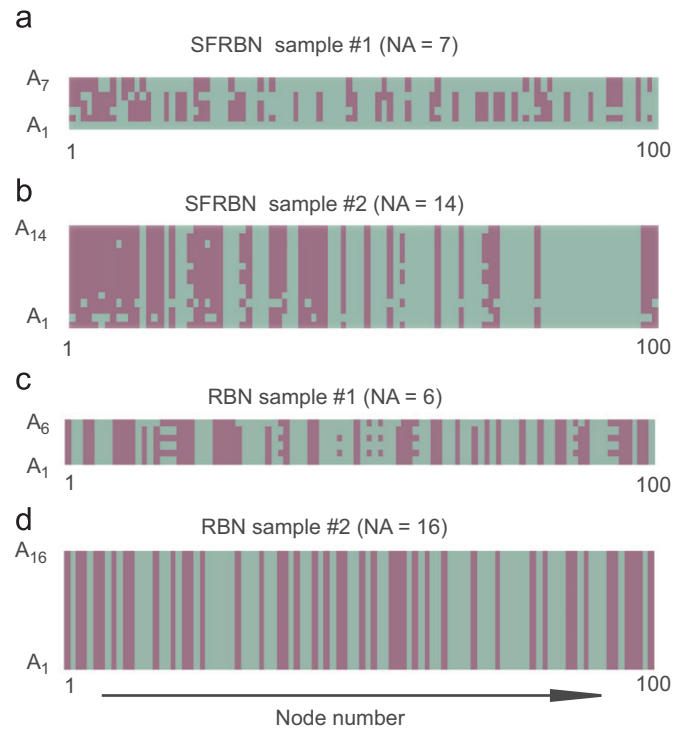
Fig. 5 shows the change of rate  $R_f(k_i)$  of frozen nodes with respect to connectivity  $k_i$  for SFRBN with  $\langle k \rangle = 2$ . We see that  $R_f(k_i)$  decreases as  $k_i$  increases in all cases with different network sizes. This tendency becomes more remarkable for a node with a larger connectivity. Fig. 5(b) shows the relationship between the growth of cycle length and the number of relevant nodes given by  $N - N_f$ . Roughly speaking, the cycle length exponentially increases with network size even when frozen nodes are excluded.

Fig. 6(a) shows the peak position  $N_f^{peak}$  as a function of network size  $N$  for SFRBN with  $\langle k \rangle = 2$ .  $N_f^{peak}$  shows a linear increase with respect to network size  $N$  such as  $N_f^{peak} \approx N/2$ . In Fig. 6(b), we show how the average of the numbers of frozen functions over 1000 different network samples,  $\langle N_{func} \rangle$ , depends on network size  $N$ .

A frozen function is defined by a Boolean function in which the state of a node is independent of input information. Accordingly, we note that a node assigned by a frozen function is automatically a frozen node. We see that the peak position may be strongly correlated with frozen functions in the system. As we expect,  $N_{func}$  increases linearly with network size  $N$  for both SFRBN with  $\langle k \rangle = 2$  and RBN with  $K = 2$ . Slopes are  $N_{func}/N = \frac{1}{8}$  for SFRBN with  $\langle k \rangle = 2$  and  $N_{func}/N = \frac{1}{3}$  for RBN with  $K = 2$ , respectively. We have to analyze the frozen nodes that arise from all canalizing

functions (Drossel, 2008). However, the reason why the peak appears around  $N_f \approx N/2 - 2N/3$  in SFRBN with  $\langle k \rangle = 2$  is not yet clear.

In Fig. 7, the distribution of the number of frozen nodes for each attractor is shown for the cases with  $\langle k \rangle = 3$  and 4. As is naively expected, the rate of frozen nodes in an attractor decreases and the peak near  $N_f \approx N$  moves to the one near  $N_f \approx 0$  as connectivity  $\langle k \rangle$  increases in both SFRBN and RBN. In particular,



**Fig. 8.** (Color online) Examples of the relationship between attractors and frozen nodes are shown for (a) and (b) SFRBNs with  $\langle k \rangle = 2$  and for (c) and (d) RBNs with  $K = 2$ , where  $N = 100$ . The vertical axis denotes attractors arranged from long cycle length to short one, while the horizontal axis denotes the node number in the high connectivity order. A point attractor consists of only a gray color.

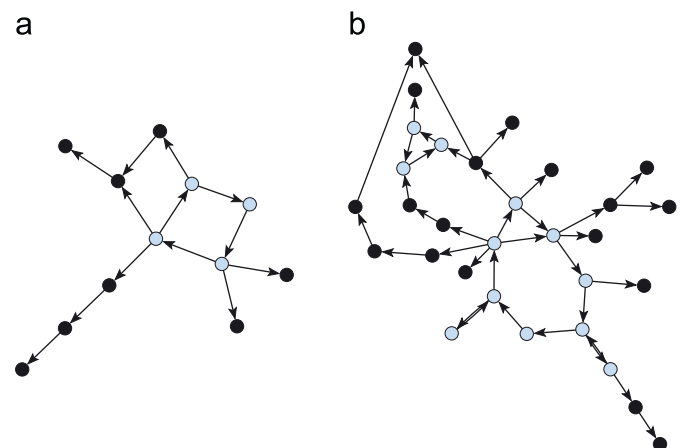


**Fig. 9.** (Color online) Unfrozen part in RBN with  $K = 2$  and  $N = 100$  is shown. Results are shown for (a) sample #2 and (b) sample #5 given in Table 2, respectively. Relevant nodes constructing a relevant loop are represented by open circles.

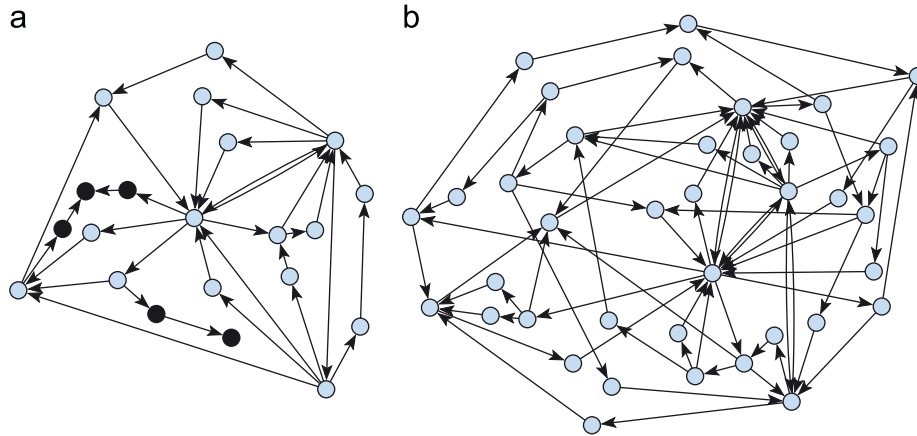


**Fig. 10.** (Color online) Unfrozen nodes in SFRBN with  $\langle k \rangle = 2$  and  $N = 100$ . Results are shown for (a) sample #2 and (b) sample #5 given in Table 2, respectively. Relevant nodes constructing relevant loops are represented by open circles. All unfrozen nodes are relevant nodes in (b).

**Table 2**

The numbers of unfrozen nodes  $N - N_f$  and of relevant nodes  $N_r$  are shown for five different network samples of RBN with  $K = 2$  and network size  $N = 100$ .

Sample	$N$	$N - N_f$	$N_r$	$N_A$
#1	100	7	2	3 (2, 1, 1)
#2	100	12	4	2 (all 8)
#3	100	14	4	4 (all 4)
#4	100	26	8	16 (all 16)
#5	100	30	12	5 (3, 3, 2, 1, 1)

The leftmost column denotes sample classification numbers.  $N_A$  is the number of attractors in the network sample. Network structures that consist of only unfrozen nodes of sample #2 and #5 are shown in Fig. 9. Numbers in bracket in the rightmost column denote periods of attractor.

**Table 3**

The numbers of unfrozen nodes  $N - N_f$  and of relevant nodes  $N_r$  are shown for five different network samples (#1 – #5) of SFRBN with  $\langle k \rangle = 2$  and network size  $N = 100$ .

Sample	$N$	$N - N_f$	$N_r$	$N_A$
#1	100	20	2	2 (2, 1)
#2	100	21	16	2 (8, 8)
#3	100	26	19	4 (16, 14, 4, 2)
#4	100	40	32	2 (7, 4)
#5	100	38	38	3 (128, 33, 2)

The leftmost column denotes sample classification numbers.  $N_A$  is the number of attractors in the network sample. Network structures that consist of only unfrozen nodes of sample #2 and #5 are shown in Fig. 10. Numbers in bracket in the rightmost column denote periods of attractor.

we can see that the distribution has a peak near  $N_f \approx N/8$  for SFRBN with  $\langle k \rangle = 3$ . We need a clear explanation for the origin of the difference between peak structures in SFRBN and RBN. It is under consideration (Kinoshita et al., 2008c).

### 3.2. Relevant loops and hub nodes

Up to now, we have statistically investigated the number of frozen nodes in a network. In this subsection, we pay our

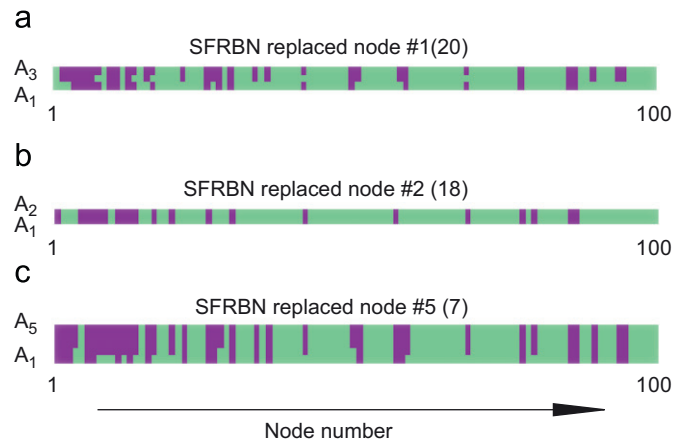


**Fig. 11.** (Color online) Examples of the relationship between attractors and frozen nodes are shown for a modified network sample #5 in SFRBN with  $\langle k \rangle = 2$  and  $N = 100$ . (See sample #5 in Table 2.) We select a highly connected node (a) #1, (b) #2, and (c) #5, and replace the originally assigned Boolean function by a frozen function. The number in the bracket denotes the input-degree of the replaced node. The vertical axis denotes the attractors arranged from a long cycle length to a short one, while the horizontal axis denotes the node number in the high connectivity order. Gray (dense) color corresponds to frozen (active) node. Point attractor consists of only gray color.

attention to the role of frozen and unfrozen nodes in each network structure.

Fig. 8 shows the relationship between each attractor and its frozen nodes. Frozen nodes of the network are fixed, independent of attractor in the cases. We investigate the role of unfrozen nodes in the network through the same typical examples.

Fig. 9 illustrates an unfrozen part such that frozen nodes and links in the network are removed from RBN with  $K = 2$  and  $N = 100$ . Here we find that there are two types of unfrozen nodes in the network. We define a directed loop that consists of links, and call a node connected with directed loops a *relevant loop node*. The majority of the nodes are frozen, and a small number of unfrozen nodes constitute relevant loops. And also the majority of the unfrozen nodes are slaved in the sense that they are not relevant nodes, i.e. irrelevant nodes (see Table 1).

Fig. 10 shows an unfrozen node is almost a relevant node for SFRBN with  $\langle k \rangle = 2$  and  $N = 100$ , on the other hand. We see that

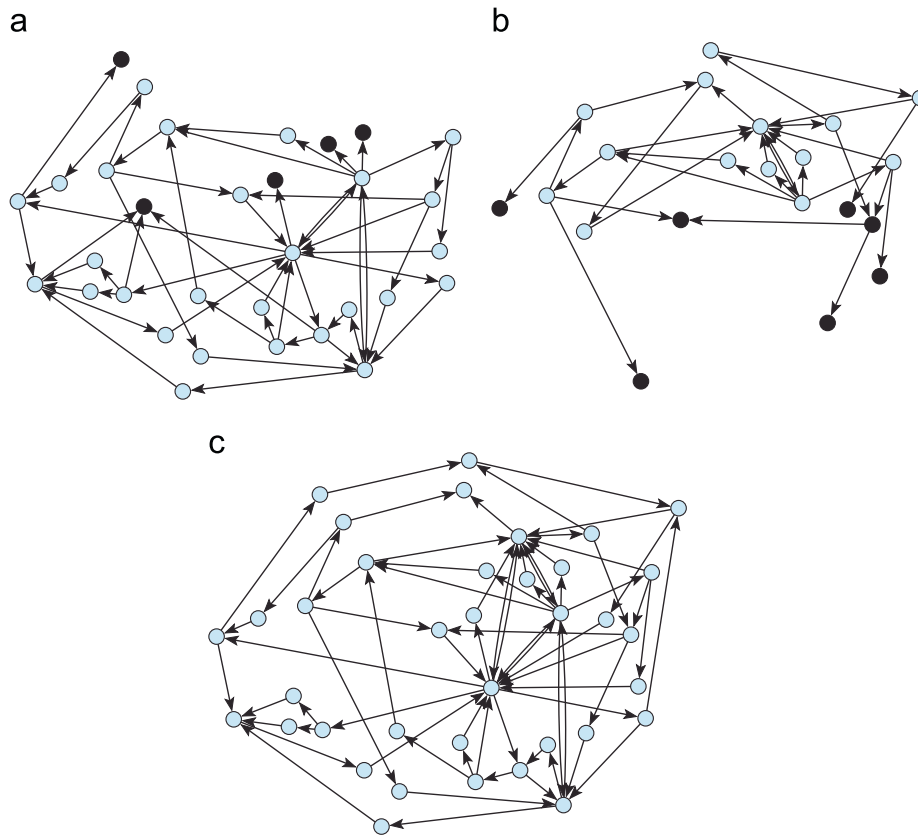


**Fig. 12.** (Color online) Unfrozen part in SFRBN with  $(k) = 2$  and  $N = 100$  is shown when a frozen function is assigned to a hub node as a Boolean function. Results are shown for replaced nodes (a) #1, (b) #2, and (c) #5, which are summarized in Table 4, respectively. Relevant nodes that construct relevant loops are shown by open circles. All unfrozen nodes are relevant nodes in (c).

**Table 4**

The numbers of unfrozen nodes  $N - N_f$  and of relevant nodes  $N_r$ , when a Boolean function assigned to a node is replaced by a frozen function in the network sample #5 in SFRBN with  $(k) = 2$ .

Node	$N - N_f$	$N_r$	$N_A$
#1(20)	32	27	3 (28, 6, 4)
#2(18)	21	14	2 (6, 3)
#5(7)	37	37	5 (18, 12, 12, 5, 2)
#7(6)	29	27	1 (12)
#9(5)	37	37	6 (92, 15, 8, 6, 2, 1)

The leftmost column denotes the number of replaced nodes.  $N_A$  is the number of attractors in the network sample. Number in bracket in the leftmost column denotes input-degree of the replaced node. Numbers in bracket in the rightmost column denote periods of attractor. Network structures that consist of only unfrozen nodes are shown for the cases of #1, #2, #5 in Figs. 12(a)–(c), respectively.

a relevant loop includes a hub node in the network for almost all cases. Moreover, we confirm that a relevant loop consists of a highly connected node as well. The result for several network samples of RBN and SFRBN is summarized in Tables 2 and 3.

In the examples, we see that the number  $N_r$  of relevant nodes in the case of SFRBN is larger than that in the case of RBN. As was mentioned in the Introduction, in general, attractor periods  $\ell_c$  in SFRBN are larger than those in RBN. Based on observation for Figs. 9 and 10, we would like to point out that the number of relevant nodes in each attractor becomes relatively large when a node with large connectivity of input-degree and one with large

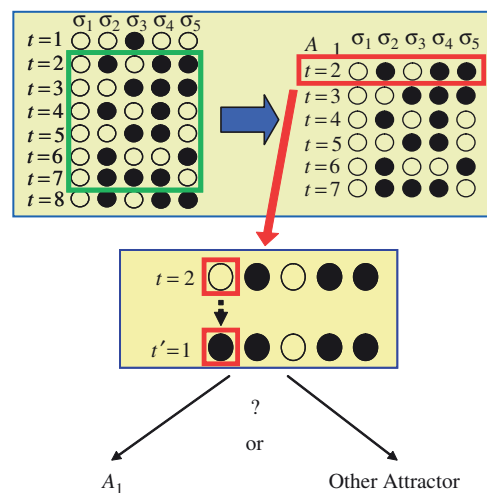


**Fig. 13.** (Color online) Robustness against a perturbation of single-node inversion is schematically shown.

output-degree are conforming to a relevant loop of the network. The above tendency in SFRBN seems to be in contrast to that in RBN because RBN has equal connectivity for all nodes.

This can be explained by the following observation: from Fig. 9, we first observe that in RBN of  $K = 2$  the degrees of input and output of a relevant node are 1 or 2 such that relevant nodes belong to simple planar loops in state space. On the other hand,

from Fig. 10, in SFRBN of  $\langle k \rangle = 2$  the degrees of input and output of a relevant node are distributed with various numbers such as 1–9, where the degree of input is almost identical to that of output for

each relevant node. The set of relevant nodes for an attractor forms a web of relevant nodes, which itself seems to be an SFRBN (i.e. a multi-dimensional loop structure). Therefore, the network

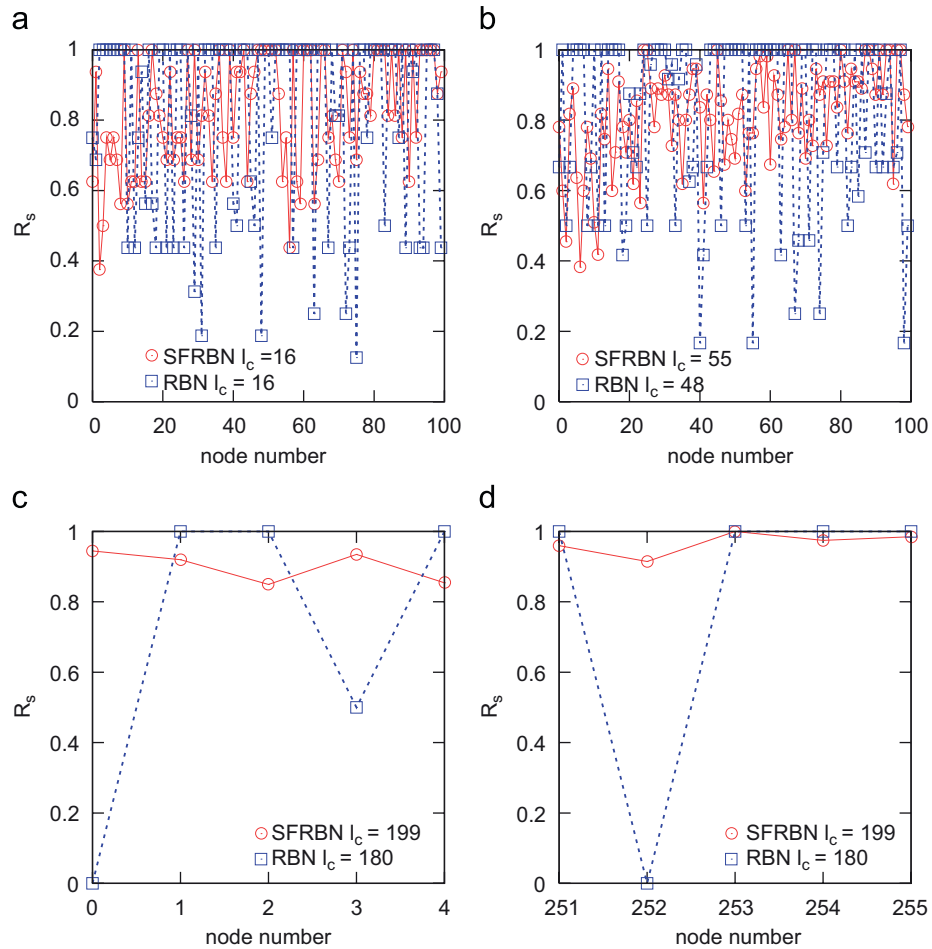


**Fig. 14.** (Color online) Rate  $R_s$  that a perturbed state returns to states in an original attractor is shown as a function of numbered node in the order of in-degree  $k_i$ . We have used the network size of  $N = 100$  in both SFRBN with  $\langle k \rangle = 2$  and RBN with  $K = 2$ . Periods of attractor are (a)  $\ell_c = 16$  in SFRBN and  $\ell_c = 16$  in RBN, (b)  $\ell_c = 55$  in SFRBN and  $\ell_c = 48$  in RBN, respectively. Panels (c) and (d) show a partial result for network size  $N = 256$ . Periods of attractor are  $\ell_c = 199$  in SFRBN and  $\ell_c = 180$  in RBN, respectively. The horizontal axis represents “node number” in the order of input-degree.

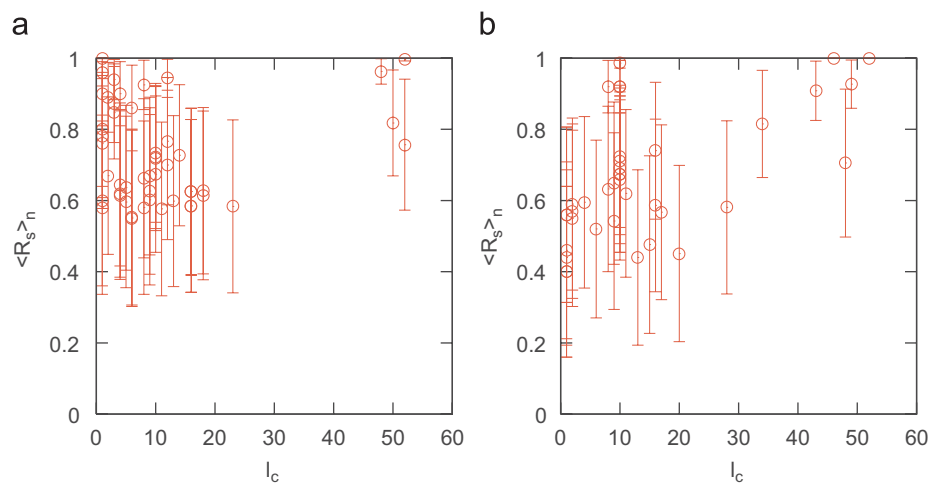


**Fig. 15.** (Color online) Averaged robustness  $\langle R_s \rangle_n$  against a single-node inversion is shown as a function of cycle length  $\ell_c$  in the (a) RBN with  $K = 2$  and (b) SFRBN with  $\langle k \rangle = 2$ , where  $N = 50$ . Bar indicates the standard deviation. Data are overplotted for several network samples of  $N = 50$ .

structure among relevant nodes in SFRBN is more complex than that in RBN. Hence, the attractor period of SFRBN has to be much longer than that of RBN.

One of the important properties in scale-free topology is the existence of a highly connected hub node such as in the yeast synthetic network and so on (Barabási et al., 1999; Barabási and Oltvai, 2004; Lee et al., 2002; Sen et al., 2003; Kauffman et al., 2003; Skarja et al., 2004; Albert, 2006). Apparently, a hub node becomes frozen, whenever a frozen function is assigned to the hub node. Here, setting a frozen function to a hub node as a Boolean function, we try to investigate the influence of frozen function on attractors of the network.

Fig. 11 shows the relationship between attractors and frozen nodes in the same network structure such as the case in Fig. 10(b),

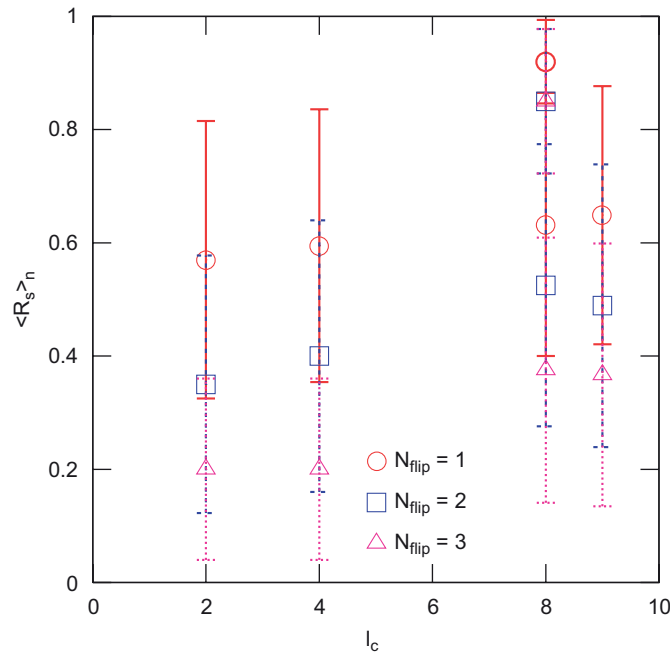


**Fig. 16.** (Color online) Averaged robustness  $\langle R_s \rangle_n$  against a single-, a double- and a triple-node inversions (which correspond to  $N_{\text{flip}} = 1, 2, 3$ , respectively) are shown as a function of cycle length  $\ell_c$  for the SFRBN with  $\langle k \rangle = 2$  and  $N = 50$ .

except that a frozen function is assigned to a hub node. Relationship between the attractor and the Boolean function in SFRBN approaches that in RBN, when frozen functions are assigned to the nodes with a larger connectivity.

Fig. 12(a) shows a network that consists of unfrozen nodes in the case. As we expect, we find that the number of relevant nodes decreases, comparing with the case of Fig. 10(b).

We have tried the same calculations for such a replacement of Boolean function for other nodes (#2, #5). They are shown in Figs. 12(b) and (c), respectively. Results for other cases are also summarized in Table 4. In all the cases, we can see that the number of unfrozen nodes and the number of relevant nodes are smaller than those without the replacement (i.e. sample #5 in Table 2). Furthermore, we see that the structure of attractor in the network drastically changes by the replacement of Boolean functions.

#### 4. Robustness of attractors

Recently, the relationship between Boolean dynamics and network topology has been investigated by many authors from the view points of stability and evolvability of network structures (Oosawa and Savageau, 2002; Aldana, 2003; Aldana et al., 2007; Fox and Hill, 2001; Serra et al., 2003; Aldana and Cluzel, 2003; Handrey et al., 2007; Gecow, 2007). In this section, we investigate robustness of an attractor to an external perturbation caused by an inversion of binary state on a node (Kinoshita et al., 2008a, b; Fretter and Drossel, 2008).

##### 4.1. Robustness of an attractor to a state inversion

We are going to study the robustness of an attractor to a state inversion. To do so, we consider returning rate  $R_s$  as an indication for robustness of an attractor. The returning rate  $R_s$  is defined as follows: (1) We seek for all attractors in a network of size  $N$ . (2) We pick up one attractor whose cycle length is  $\ell_c$ , which means that there are  $\ell_c$  time steps to return to the initial state. By definition, the attractor consists of at most  $\ell_c$  distinct states in the cycle. (3) For such states belonging to the attractor, we pick up a node in the network system and change the state on the node as a single-node perturbation at a time  $t_i$  within  $\ell_c$  time steps (i.e.  $t_i \in [1, \ell_c]$ ). (4) After that, we monitor to which attractor the

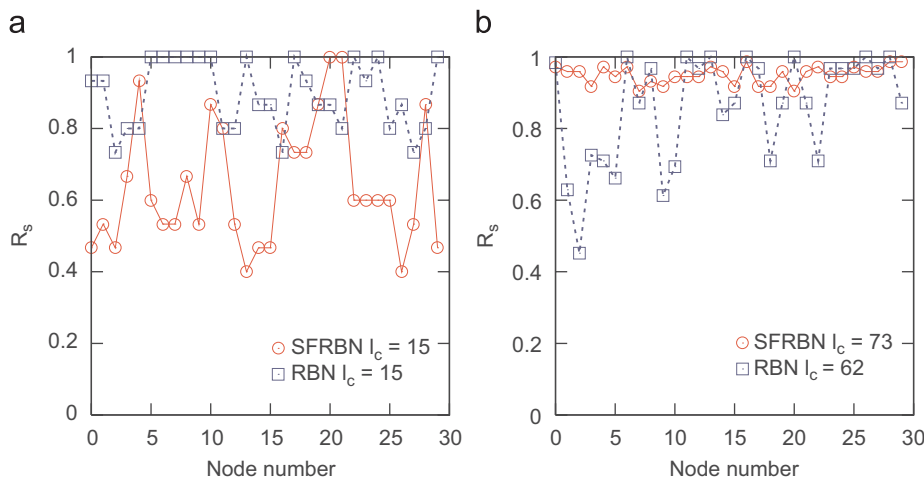


**Fig. 17.** (Color online) (a) Robustness  $R_s$  is shown as a function of node number for some attractors of SFRBN with  $\langle k \rangle = 3$  and RBN with  $K = 3$  in network size of  $N = 30$ . Periods of attractor are  $\ell_c = 15$  for SFRBN and  $\ell_c = 15$  for RBN, respectively. (b) Robustness  $R_s$  is shown as a function of node number for some attractors of SFRBN with  $\langle k \rangle = 4$  and RBN with  $K = 4$  in network size of  $N = 30$ . Periods of attractor are  $\ell_c = 73$  for SFRBN and  $\ell_c = 62$  for RBN, respectively.

perturbed state of the whole network belongs. In other words, as a result of perturbation, the trajectory of the attractor may leap from the trajectory of the original attractor to another one, i.e. the *attractor shift* (see Fig. 13). We would like to know whether or not the perturbed state remains in the original attractor. (5) We redo the same procedure for all times  $t_i$  in the  $\ell_c$  time steps. We define a returning rate  $R_s(i)$  that the state perturbed at the  $i$ th node returns to a state in the original attractor by a ratio between the number  $N_{ret}$  of returning states and the total number  $\ell_c$  of the states such as  $R_s(i) = N_{ret}/\ell_c$ . (6) We repeat the above procedure from (1) through (5), with changing the perturbed node to run over all nodes of the network. (7) Furthermore, we can define the averaged returning rate  $\langle R_s \rangle_n$  by the average of  $R_s$  over all the nodes in the network such as  $\langle R_s \rangle_n = (1/N) \sum_{j=1}^N R_s(j)$ . (8) And as we will use in Section 5, we are able to define the averaged returning rate of  $\langle R_s(i) \rangle_a$  by the average over all the attractors in the network as  $\langle R_s(i) \rangle_a = (1/N_A) \sum_{s=1}^{N_A} R_s(i)$ , where  $N_A$  is the total number of attractors in the system.

Fig. 14(a) shows the variation of  $R_s$  on each node for an attractor with  $\ell_c = 16$  for SFRBN and  $\ell_c = 16$  for RBN, respectively. Similarly, Fig. 14(b) shows the variation of  $R_s$  on each node for an attractor with  $\ell_c = 55$  for SFRBN and  $\ell_c = 48$  for RBN, respectively. We see that the number of “sensitive nodes” (i.e.  $R_s < 1$ ) in SFRBN is much larger than that in RBN. On the other hand, in RBN, a perturbation to an active node influences effectively the attractor shift ( $R_s < 0.6$ ), although the number of sensitive nodes is not so large. Therefore, in SFRBN, a perturbation to a highly connected hub may give rise to an attractor shift much easier than a perturbation to a less connected node. In Figs. 14(c) and (d), we

show a partial result for attractors with large periods of  $\ell_c = 199$  in SFRBN and  $\ell_c = 180$  in RBN for a large network of  $N = 256$ . We note that the same characteristics is confirmed even for other cases.

Fig. 15 shows the averaged robustness  $\langle R_s \rangle_n$  over all nodes as a function of cycle length in the case of a single-node inversion. We see that the  $\langle R_s \rangle_n$  for an attractor with a long cycle length is relatively large value, which means that the attractor is robust against a single-node inversion. The tendency is more eminent in SFRBN with  $\langle k \rangle = 2$  than in RBN with  $K = 2$ .

We then consider robustness of an attractor against a randomly selected multi-node inversion. Fig. 16 shows the averaged robustness of some attractors in SFRBN with  $\langle k \rangle = 2$ . As we expect, a multi-node state inversion is more significant for the attractor shift than a single-node inversion.

We further study how the connectivity effects the robustness of an attractor under a single-node inversion. Fig. 17 shows the robustness  $R_s$  for some attractors in SFRBN with  $\langle k \rangle = 3, 4$  and in RBN with  $K = 3, 4$ , where network size is  $N = 30$ . The behavior of  $R_s$  is the same as that in the case with  $\langle k \rangle = 2$ . As Fig. 18 shows, we can confirm that an attractor with a higher connectivity in the network are less robust against a single-node inversion in both RBN and SFRBN.

#### 4.2. Transition diagram between attractors

Homeostatic stability is high when attractors behave independently in order not to reach one another among different

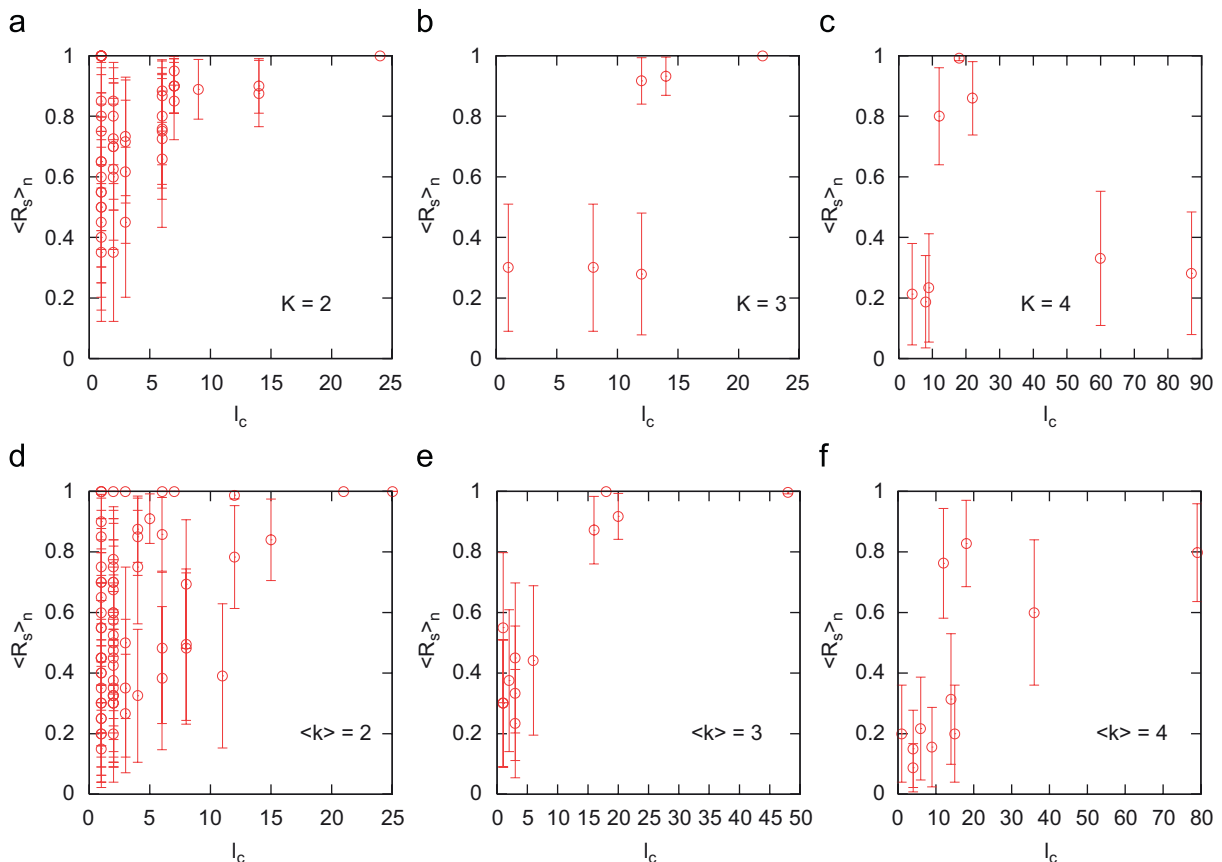
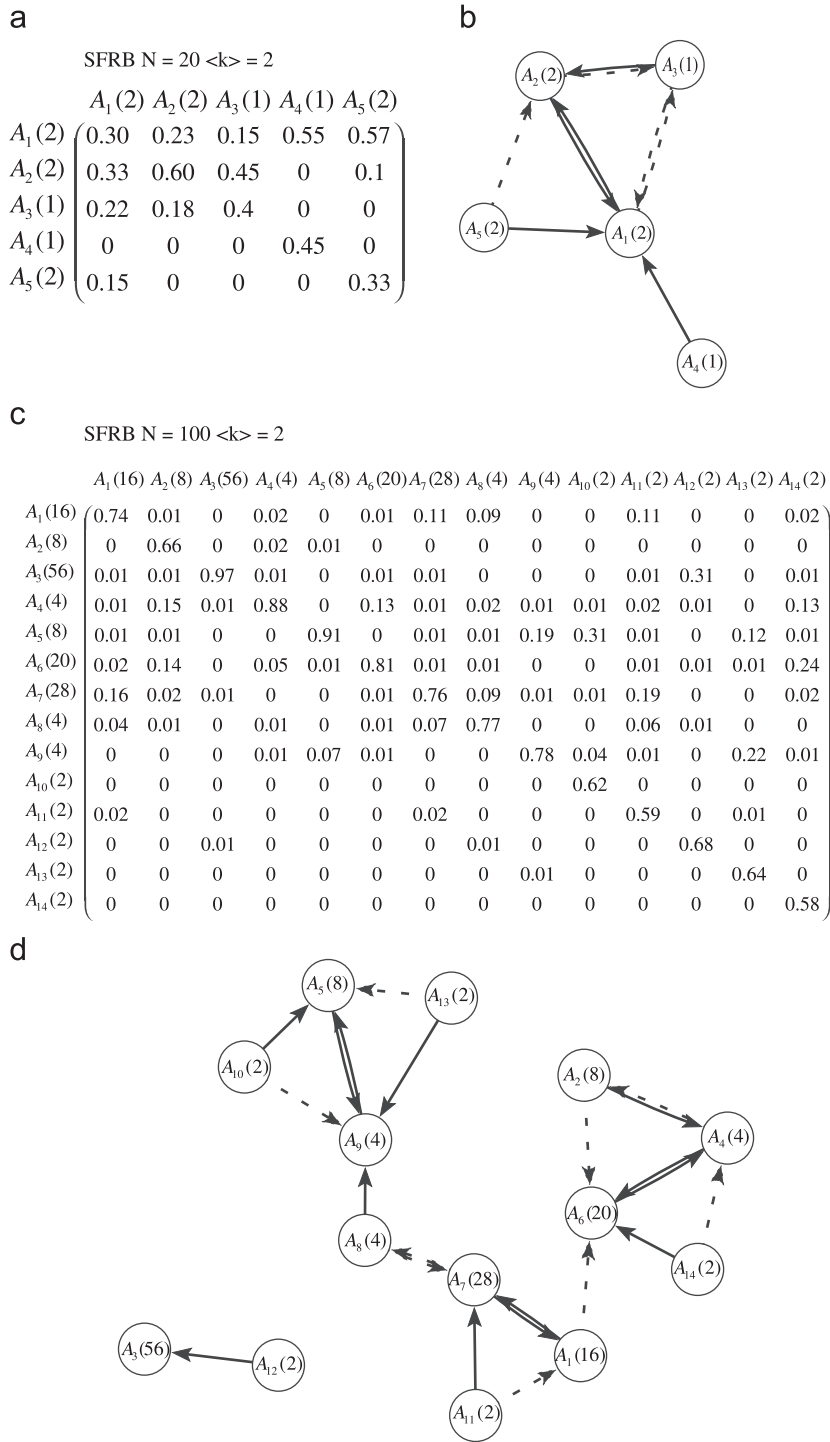


Fig. 18. (Color online) Averaged robustness  $\langle R_s \rangle_n$  against a single-node inversion is shown as a function of cycle length  $\ell_c$  for RBNs with (a)  $K = 2$ , (b)  $K = 3$ , and (c)  $K = 4$ , and SFRBNs with (d)  $\langle k \rangle = 2$ , (e)  $\langle k \rangle = 3$ , (f)  $\langle k \rangle = 4$ , where  $N = 20$ .



**Fig. 19.** (a) Examples for transition probability matrix and transition diagram are shown for SFRBN with  $\langle k \rangle = 2$  and  $N = 20$  [(a) and (b)] and  $N = 100$  [(c) and (d)]. A solid arrow between two attractors represents the most possible transition from the perturbed attractor to the other one, where the direction of transition is indicated by the direction of arrow. On the other hand, dotted arrows represent the second most probable transitions. Number in bracket for attractor denotes cycle length  $\ell_c$  of attractor such as  $A_i(\ell_c)$ . Attractor  $A_1$  stands for the most stable attractor against the perturbation.

attractors. This is directly related to the basin structure of the Boolean dynamics in the network, where the basin structure means a structure of the set of attractors and their basins of attraction in state space. Robustness against a perturbation can partially reveal a basin structure among attractors.

In Figs. 19(a) and (c), we show a typical example of transition probability matrix between four attractors ( $A_1, A_2, A_3, A_4$ ) under a

perturbation given as a single-node inversion, where SFRBN with  $\langle k \rangle = 2$  and  $N = 50$  is studied. A schematic diagram based on the matrix is given in Figs. 19(b) and (d). Magnitude of matrix element  $p_{ij} \equiv P(A_i \rightarrow A_j)$  represents a transition probability between attractors  $A_i$  and  $A_j$ . For example, in Fig. 19(b), the attractors can be classified into stable and unstable attractors, based on the robustness of the attractor against a perturbation. A stable

attractor remains in the same attractor with a high probability. On the other hand, an unstable attractor  $A_3(A_4)$  mainly flows into a stable attractor  $A_2(A_1)$ . There are a few unstable attractors with a large period  $\ell_c$ , and an attractor with the largest  $\ell_c$  is not always most stable in the network.

Fig. 20 shows schematically some typical diagrams of transition probability between attractors  $A_i$  for SFRBN with  $\langle k \rangle = 3, 4$ . From Figs. 19 and 20, it is evident that an attractor with the largest period is most stable against a perturbation. It has a wide attractive domain. On the other hand, an attractor with a small period  $\ell_c$  is unstable against a perturbation, in general. In the network examples of Fig. 20, all attractors flow into attractor  $A_1$  with the largest period in the network.

Moreover, we find that the variation in attractor period for RBN is smaller than that for SFRBN. In other words, among attractors in SFRBN, the size of a basin of attraction is not so different from that of other basin of attraction. And it is not so in RBN. Such a property directly influences entropy of the system.

4.3. Basin entropy and transition between attractors

Recently, Krawitz and Shmulevich (2007b) found that the basin entropy for RBN with  $K = 2$  increases with network size  $N$  (Nykter et al., 2008). This entropy seems important and

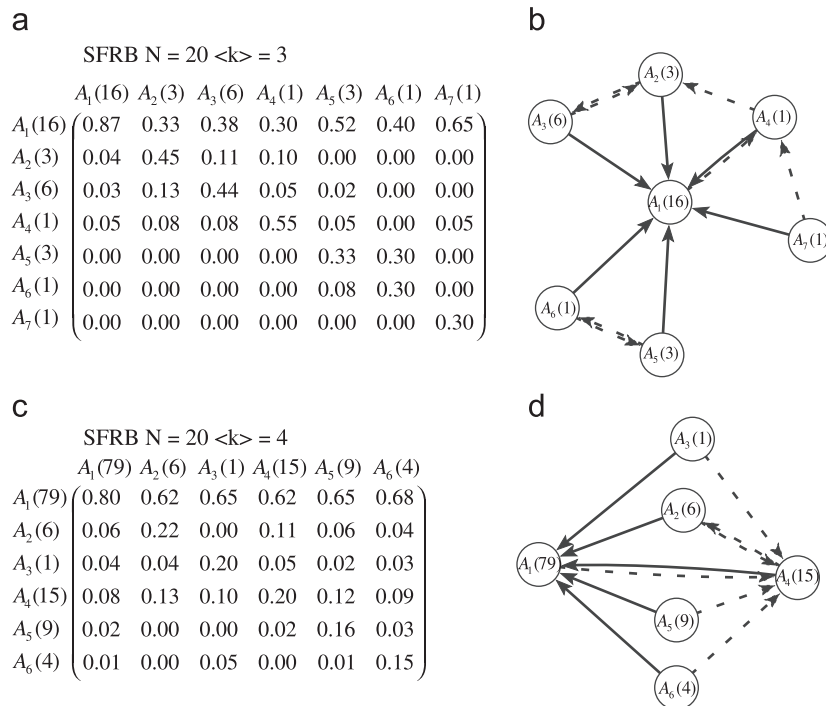


Fig. 20. (Color online) Examples for transition probability matrix [(a) and (c)] and transition diagrams [(b) and (d)] are shown for SFRBN with  $\langle k \rangle = 3, 4$  and  $N = 20$ . A solid arrow between two attractors represents the most possible transition from the perturbed attractor to the other one, where the direction of transition is indicated by direction of arrow. On the other hand, dotted arrows represent the second most probable transitions. Number in bracket for attractor denotes cycle length  $\ell_c$  of attractor such as  $A_i(\ell_c)$ . Attractor  $A_1$  stands for the most stable attractor against the perturbation.

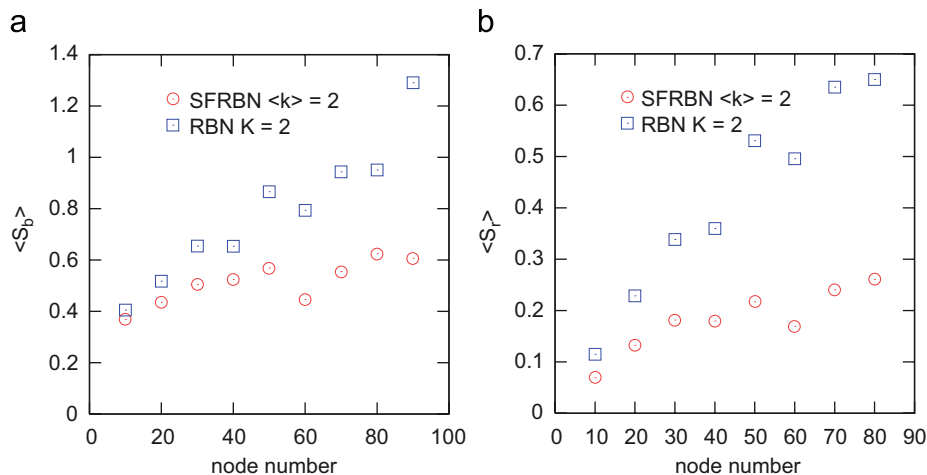


Fig. 21. (Color online) (a) Averaged basin entropy  $\langle S_b \rangle$  over 100 network samples is shown as a function of network size  $N$  up to  $N = 100$  are shown for RBN with  $K = 2$  and SFRBN with  $\langle k \rangle = 2$ . (b) Averaged relative entropy  $\langle S_r \rangle$  over 80 network samples is shown as a function of network size  $N$ .

relevant for our study on SFBRN. So, let us now consider an entropy that characterizes attractors in the Boolean dynamics on a network.

Let us first define the *basin entropy*  $S_b$  of the network by

$$S_b = - \sum_{i=1}^{N_A} P_i \log P_i, \quad (2)$$

where  $N_A$  is the total number of attractors,  $P_i$  the fraction of state space occupied by basin of attraction of attractor  $A_i$  and  $\sum_{i=1}^{N_A} P_i = 1$ . Basin entropy reflects on the distribution of area belonging to a basin of attraction of each attractor in RBN and SFRBN. In general, we determine an approximated probability  $P_i$  by a randomly selected initial state in state space, although we can exactly determine  $P_i$  for all the attractors in a relatively small network. In a network, the larger the basin entropy, the more uncertainty the dynamical behavior is and the more enhanced the effective complexity is. We note that the average of entropy over a network ensemble is necessary in order to get a definite property.

In Fig. 21(a), for both RBN with  $K = 2$  and SFRBN with  $\langle k \rangle = 2$ , we show the *averaged basin entropy* ( $S_b$ ) over 100 network samples monotonically increases as network size  $N$  increases. The averaged basin entropy for RBN is larger than that for SFRBN, because the distribution of sizes of basin of attraction for RBN is relatively more uniform than that for SFRBN.

Next, let us define the *relative entropy*  $S_r$  of the transition between attractors as (Billingsley, 1960; Akashi, 1999)

$$S_r = \sum_{i=1}^{N_A} P_i \sum_{j=1}^{N_A} p_{ij} \log \frac{p_{ij}}{Q_j}, \quad (3)$$

where  $p_{ij}$  are elements of transition probability matrix, and we hold  $\sum_{j=1}^{N_A} p_{ij} = 1$ . Here  $Q_j$  is the probability that is transferred from  $P_j$ , which is defined by  $Q_j = \sum_{i=1}^{N_A} p_{ji} P_i$ , and  $\sum_{j=1}^{N_A} Q_j = 1$  since  $\sum_{j=1}^{N_A} p_{ji} = 1$  is guaranteed. We give a brief explanation for the relative entropy in Appendix B.

In Fig. 21(b), we show the averaged relative entropy ( $S_r$ ) as a function of network size  $N$  for some RBN with  $K = 2$  and SFRBN with  $\langle k \rangle = 2$ . We show that the averaged relative entropy for SFRBN with  $\langle k \rangle = 2$  is smaller than that for RBN with  $K = 2$ . This does not mean the vulnerability of SFRBN with  $\langle k \rangle = 2$ , since we can interpret that the attractor transition responds more flexibly to a perturbation in SFRBN with  $\langle k \rangle = 2$ . Furthermore, we find that the averaged relative entropy increases with network size  $N$  for RBN with  $K = 2$ , while it is saturated to a certain value for SFRBN with  $\langle k \rangle = 2$ .

We have investigated relatively small networks of  $N \leq 60$  in order to obtain attractor transitions. We note that it is NP-hard to find an attractor even for an attractor with a short period (Zhang et al., 2007). Indeed, elapsed time exponentially increases as a function of network size  $N$  even for RBN with

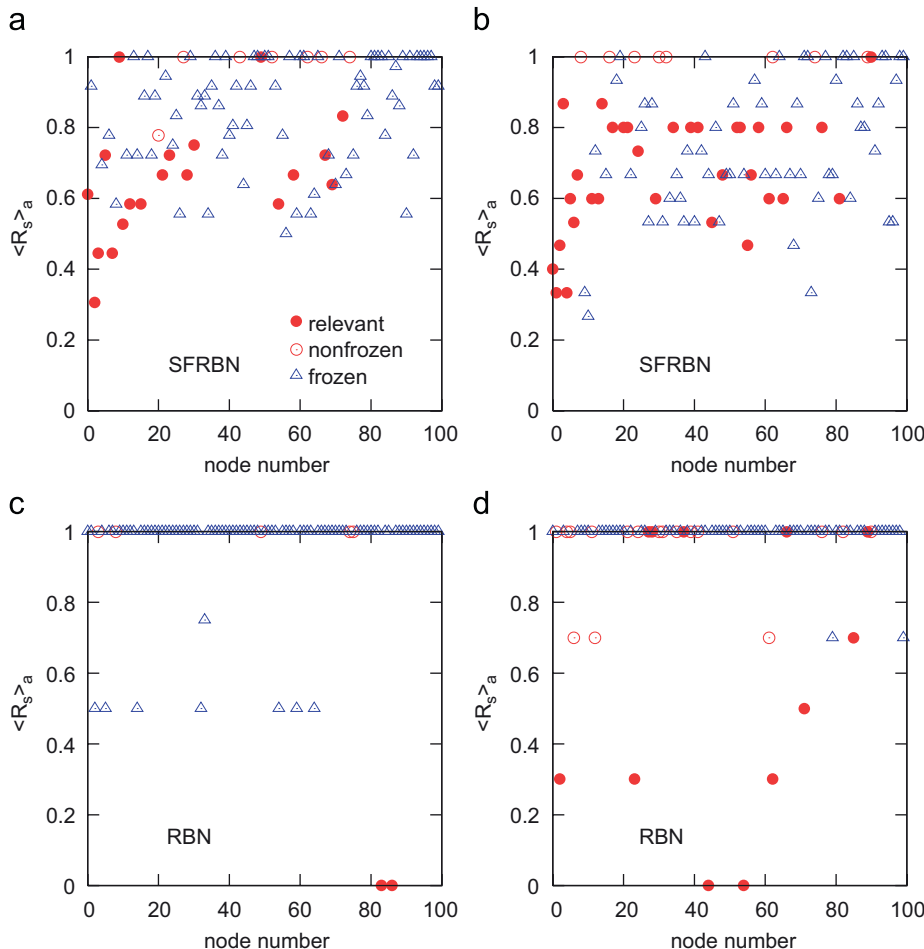


**Fig. 22.** (Color online) Averaged robustness ( $R_s$ )<sub>a</sub> over all attractors against a single-node perturbation. Distinction between frozen (triangle) and unfrozen (circle) nodes is shown. Panels (a) and (b) show a result of the two network samples in SFRBN with  $\langle k \rangle = 2$  and  $N = 100$ . Panels (c) and (d) show a result of the two network samples in RBN with  $K = 2$  and  $N = 100$ . A relevant node is represented by a filled circle.

$K = 2$ . As shown in Figs. 1(a) and (b), it is much more difficult to find all attractors in a given SFRBN than in a given RBN, because it takes much computational time to find an attractor with a long period. This is due to inhomogeneity of basin size of attractor. A huge amount of computational time is necessary in order to obtain an accurate information for transitions between attractors in a large network. We need further study to explore the details of this issue, and we leave it as an open question for future research.

## 5. Relationship between robustness and frozen nodes

In this section, we consider the relationship between robustness and frozen nodes, which has been investigated in the previous sections.

In Fig. 22, we show changes in the averaged returning rate  $\langle R_s(i) \rangle_a$  over all attractors under a perturbation at each node  $i$  for SFRBN with  $\langle k \rangle = 2$  and for RBN with  $K = 2$ . We note here that  $\langle R_s(i) \rangle_a$  is different from  $\langle R_s \rangle_n$ ; the former is averaged over attractors, while the latter is averaged over nodes, as introduced in Section 4. Fig. 22 is basically the same as Fig. 14, except that nodes are labelled by different markers that indicate whether the node is either frozen or unfrozen or relevant. On the other hand, Figs. 23 and 24 show robustness  $R_s(i)$  for each

attractor corresponds to the results in Figs. 22(a) and (c), respectively. From Fig. 23, we see that  $R_s(i)$  for an attractor with a long period is almost the same as  $\langle R_s \rangle_n$ . Robustness property of an attractor with a short period in SFRBN is similar to that in RBN.

As is shown in some spatio-temporal diagrams in Figs. 2 and 8, we would like to note that frozen nodes are common for all attractors in the network structure, while relevant nodes are not always common for every attractor. We find that an unfrozen node (in particular, a relevant node) is more sensitive to a perturbation than a frozen node. Moreover, a relevant node with a larger input-degree are more sensitive to the perturbation than the nodes with a small input-degree. This fact shows that relevant nodes play an important role for construction of an attractor in the network. Moreover, almost the same thing is applicable to SFRBNs with  $\langle k \rangle = 3$  and  $\langle k \rangle = 4$  (see Fig. 25).

## 6. Summary and discussion

In summary, we have studied the Boolean dynamics of the Kauffman model with directed SFRBN, comparing with directed RBN for relatively small network size. In this study, we have investigated intrinsic properties of an attractor in the network in order to stem out a difference between RBN and SFRBN. For this

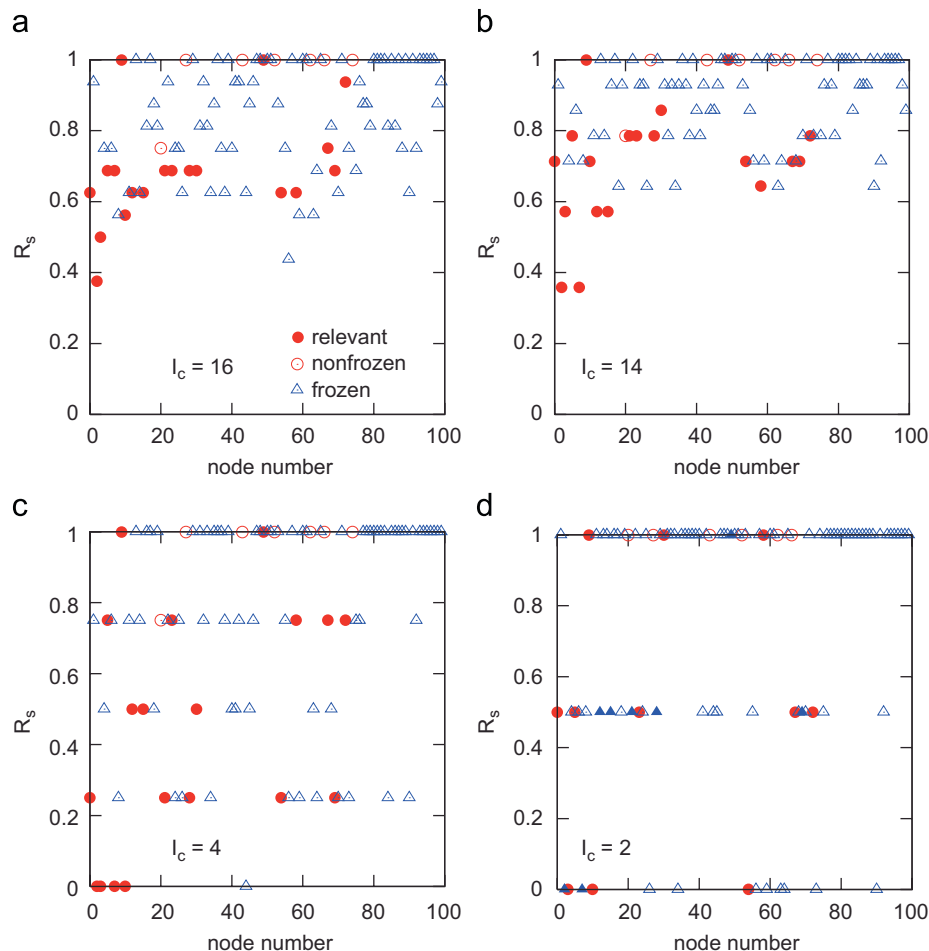


**Fig. 23.** (Color online) Robustness  $R_s(i)$  for a single-node perturbation with the distinction between frozen (triangle) and unfrozen (circle) nodes of an attractor is shown. Panels show a result for each attractor in the case of Fig. 22(a) in SFRBN with  $\langle k \rangle = 2$  and  $N = 100$ . (a)  $l_c = 16$ , (b)  $l_c = 14$ , (c)  $l_c = 4$  and (d)  $l_c = 2$ . A relevant node is shown by a filled circle, and a relevant frozen node is represented by a filled triangle.

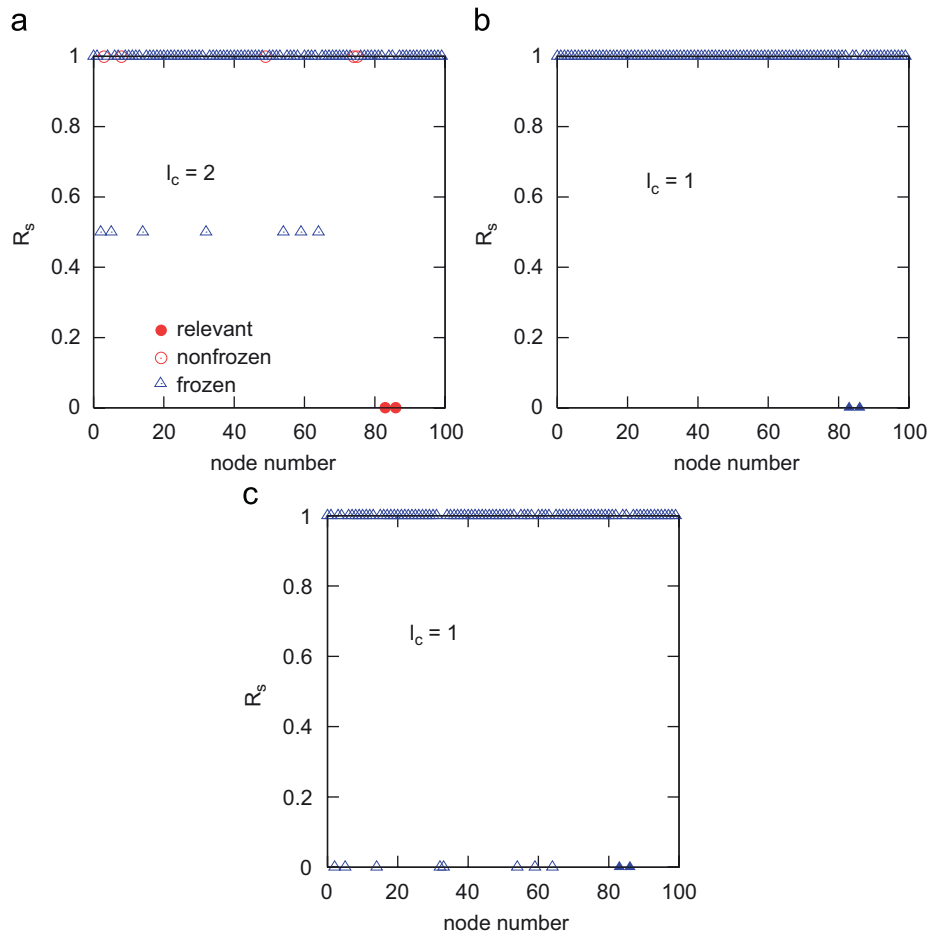


**Fig. 24.** (Color online) Robustness  $R_s(i)$  for a single-node perturbation with the distinction between frozen (triangle) and unfrozen (circle) nodes is shown. Panels show a result for each attractor in the case of Fig. 22(c) in RBN with  $K = 2$  and  $N = 100$ . (a)  $\ell_c = 2$ , (b)  $\ell_c = 1$ , and (c)  $\ell_c = 1$ . A relevant node is shown by a filled circle. A relevant frozen node is represented by a filled triangle.

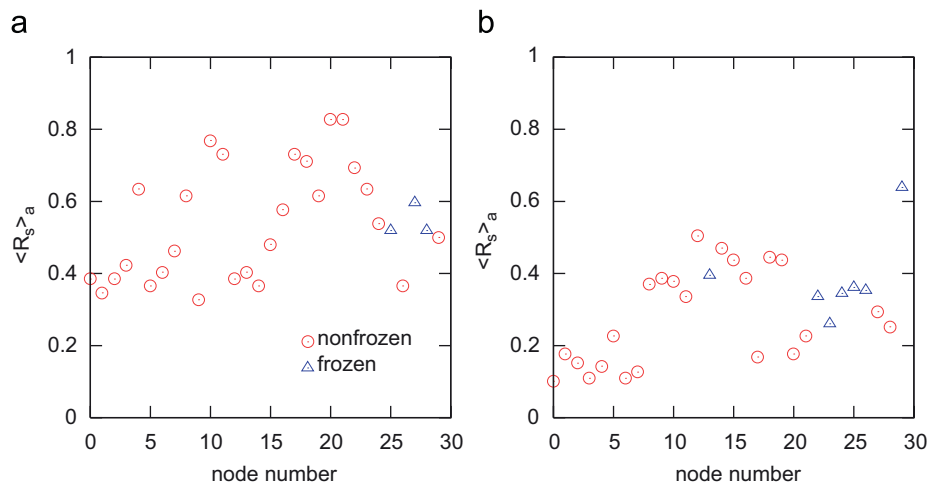


**Fig. 25.** (Color online) Averaged robustness  $\langle R_s \rangle_a$  over all attractors against a single-node perturbation is shown for SFRBN with (a)  $\langle k \rangle = 3$  and (b)  $\langle k \rangle = 4$  and  $N = 30$ . Distinction between frozen and unfrozen nodes is denoted by triangles ( $\Delta$ ) and circles ( $\circ$ ), respectively. The number of attractors in networks with  $\langle k \rangle = 3$  and 4 is given as  $N_A = 4$  ( $\ell_c = 18, 17, 15, 2$ ) and  $N_A = 5$  ( $\ell_c = 56, 21, 19, 15, 8$ ).

purpose, we have focused on frozen nodes and robustness against a perturbation. We have obtained the following results:

- (i) The total number of frozen nodes in SFRBN is smaller than that in RBN (see Fig. 4). This is reflected from a fact that cycle lengths in SFRBN are much more widely distributed than in

RBN (see Fig. 1). The majority of the nodes are frozen, and a small number of unfrozen nodes constitute relevant loops in RBN with  $K = 2$  and  $N = 100$ .

- (ii) In SFRBN with  $\langle k \rangle = 2$  and  $N = 100$  unfrozen nodes are almost relevant nodes, and a relevant loop includes a hub node in the network for almost all cases (see Fig. 10).

A relevant loop consists of a highly connected node. The number of relevant nodes in each attractor becomes relatively large when a node with a large input-degree and a large output-degree become a member of relevant nodes for the same attractor in the network. On the other hand, a RBN has no special nodes and contains a relatively small relevant loop.

- (iii) A remarkable peak around  $N/2 - 2N/3$  appears in SFRBN of  $\langle k \rangle = 2$  (see Fig. 4). Rate of frozen nodes for an attractor decreases and the peak near  $N_f \approx N$  moves to the one near  $N_f \approx 0$  as the connectivity  $\langle k \rangle$  increases in both SFRBN and RBN (see Fig. 7). In particular, we have found that the distribution has a peak near  $N_f \approx N/8$  in SFRBN of  $\langle k \rangle = 3$  (see Fig. 6). On the other hand, there is no peak around  $N/2$  in RBN of  $K = 2$  (see Fig. 4).
- (iv) Attractors can be classified into stable and unstable ones, based on robustness against a perturbation. The attractor with the largest period is the most stable against a perturbation. The variation of cycle periods of attractor in RBN is smaller than that in SFRBN. In other words, among attractors, sizes of basins of attraction in SFRBN are not so different from one another, compared to those in RBN. It is interesting to study the change in the behavior of median or mean value over a partial ensemble that consists of only relatively stable attractors in the system.
- (v) An attractor becomes more robust against a perturbation as the average number  $\langle k \rangle$  of input-degree increases, because a state inversion of a highly connected node strongly influences on the attractor shift in both RBN and SFRBN.
- (vi) The averaged basin entropy for RBN with  $K = 2$  is larger than that for SFRBN with  $\langle k \rangle = 2$ . The reason is that the distribution of sizes of basin of attraction for the case of RBN is relatively more uniform than that for the case of SFRBN.
- (vii) The averaged relative entropy for SFRBN with  $\langle k \rangle = 2$  is smaller than that for RBN with  $K = 2$ . For RBN with  $K = 2$ , the averaged relative entropy increases with network size  $N$ , while it is saturated to a certain value for SFRBN with  $\langle k \rangle = 2$ . The attractor transition responds more flexibly to the perturbation for SFRBN with  $\langle k \rangle = 2$  than it does in RBN with  $K = 2$ .

Robustness against a genetic mutation and an environmental perturbation is one of the universal features in biological systems. As we have explained in this paper, there is a tendency that the larger the cycle length of attractor, the more the robust against a perturbation of state inversion. As was seen in the relationship between biodiversity and stability in ecological systems, the stability tends to decrease as the interaction becomes complex (May, 1999; Haydon, 2000; Jansen and Kokkoris, 2003; Kondoh, 2003; Anderson and Jensen, 2005; Klemm and Bornholdt, 2005; Levin, 2000). Thus, we would like to mention that the problem between network topology and stability of attractor states is a very delicate one (Wagner, 2005; Braunewell and Bornholdt, 2007; Szejka and Drossel, 2007; Bornholdt and Sneppen, 2000; Jansen and Kokkoris, 2003), however. To confirm the precise relationship between network topology and stability, we need more accurate numerical data obtained from larger networks or more realistic networks.

In this study we have used SFRBN by considering the distribution of connectivity as a remarkable feature of the network structure. However, we can expect that a feedback loop structure strongly dominates the dynamical behavior of attractors in directed networks (Bianconi and Marsili, 2006; Bianconi et al.,

2008). Recently, an interesting network model, the so-called *feedback network*, has been proposed by White et al. (2006). Feedback networks are able to model appropriately autocatalytic chemical reaction, kinship, and so on. Because node selection, search distance and search path of network are controlled by parameters for attachment, distance decay and cycle formation parameters. Therefore, it is very interesting to study the Boolean dynamics in the feedback networks from the point of view of frozen nodes and robustness. The details about the relationship between frozen nodes and robustness against a perturbation will be published elsewhere (Kinoshita et al., 2008c).

## Acknowledgments

We would like to thank professor Masaki Goda for encouragement and discussion on this study. K.I. would like to thank Kazuko Iguchi for her continuous financial support and encouragement.

## Appendix A. Networks with scale-free topology

As is very well known (Kauffman, 1993), the network topology of RBN with connectivity  $K$  consists of  $N$  randomly connected nodes, each of which has  $K$  input-degree (i.e. in-degree). In this case, the distribution of in-degrees is given by a  $\delta$ -function distribution of  $P(k) = \delta(k - K)$ , while the output-degree distribution (i.e. the distribution of out-degrees) follows a Poissonian distribution. On the other hand, it is known that the network topology of SFRBN is very different from that of RBN. To investigate the difference in the Boolean dynamics between RBN and SFRBN, we have to be able to generate a well-defined SFRBN for each numerical calculation. To construct such a definite SFRBN, we adopt the Albert and Barabási (2000, 2002) model as follows. We consider the connected nodes as a seed in order to construct a network with scale-free topology. When we add one node to a previously existing network, new  $k$  input links are randomly chosen, accordingly to the preferential attachment probability for the network as

$$\Pi_i = \frac{k_i}{\sum_j k_j}. \quad (\text{A.1})$$

We do the same thing for output links, and we continue the above procedure until the network size  $N$  is achieved. Then for large  $N$ , the statistical distributions of in- and out-degrees follow an inverse power-law as

$$P(k) \propto \frac{1}{k^3} \quad (\text{A.2})$$

for  $1 \leq k \leq N$  and  $P(k) = 0$ , otherwise. We note that the degree distribution is one of the characteristics of the network such as the clustering coefficient (Albert and Barabási, 2002; Newman, 2002; Boccaletti et al., 2006), the centrality (Holme and Ghoshal, 2006), the modularity (Watts and Strogatz, 1998), neighborhood property (Andrade et al., 2006) and the load distribution (Goh et al., 2001), etc.

## Appendix B. Relative entropy

In this appendix, we give a brief introduction of the relative entropy that is commonly used in many fields such as information communication theory (Billingsley, 1960; Akashi, 1999) and bioinformatics (Mount, 2004), etc.

Denote by  $X$  a discrete random variable with outcome  $\{x_1, x_2, \dots, x_n\}$ , which occurs with probability distributions of

$\{P(x_1), P(x_2), \dots, P(x_n)\}$  where  $P(x_i) > 0$ ,  $i = 1, 2, \dots, n$ . Denote by  $Y$  a discrete variable with outcome  $\{y_1, y_2, \dots, y_m\}$ , which occurs with probability distributions of  $\{P(y_1), P(y_2), \dots, P(y_m)\}$  where  $P(y_j) > 0$ ,  $j = 1, 2, \dots, m$ . The  $\{P(x_i)\}$  and  $\{P(y_j)\}$  are regarded as the input and output signals in information communication theory, respectively. Let  $P_{ij} \equiv P(X = x_i, Y = y_j)$  be the probability for the joint occurrence of  $x_i$  and  $y_j$ . Using such joint probabilities, the entropy of joint events is defined by  $H(x, y) = -\sum_{i,j} P_{ij} \log P_{ij}$ . We then define the conditional probability  $P_{ij} \equiv P(y_j|x_i)$  that  $Y$  has a value  $y_j$  when  $X$  has a value  $x_i$ . Now we are able to define the transition matrix  $A$ :

$$A \equiv \begin{pmatrix} P(y_1|x_1) & P(y_2|x_1) & \cdots & P(y_m|x_1) \\ P(y_1|x_2) & P(y_2|x_2) & \cdots & P(y_m|x_2) \\ \vdots & \vdots & \ddots & \vdots \\ P(y_1|x_n) & P(y_2|x_n) & \cdots & P(y_m|x_n) \end{pmatrix}. \quad (\text{B.1})$$

Let us assume that the probability distribution  $P(y_j)$  is related to  $P(x_i)$  as

$$P(y_j) = \sum_{i=1}^n P(y_j|x_i)P(x_i), \quad j = 1, 2, \dots, m. \quad (\text{B.2})$$

Moreover, we define the *conditional relative entropy*  $I(x_i|Y)$  for the distribution  $\{P(y_j)\}$  under the condition that  $X$  takes a value  $x_i$  as

$$I(x_i|Y) = \sum_{j=1}^m P(y_j|x_i) \log \frac{P(y_j|x_i)}{P(y_j)}. \quad (\text{B.3})$$

Then, the *relative entropy* between the input variable  $X$  and the output variable  $Y$  is define as

$$I(X|Y) = \sum_{i=1}^n P(x_i)I(x_i|Y). \quad (\text{B.4})$$

We are able to interpret the relative entropy as an information capacity that indicates the accuracy of the transferred information from input signal to output signal through the transition matrix  $A = (P_{ij})$ . We call the transition matrix the “channel” in information theory.

In Section 4.3, we have calculated the relative entropies for the transitions between the attractors in SFRBN with  $\langle k \rangle = 2$  and those in RBN with  $K = 2$ , respectively. We can obtain the relative entropy  $I(A|A)$  for the transitions between attractors by a simple correspondence as  $P(x_i) \rightarrow P_i \equiv P(A_i)$ ,  $P(y_j|x_i) \rightarrow p_{ij} \equiv p(A_i \rightarrow A_j)$  and  $n = m = N_A$ .

## References

Akashi, S., 1999. Entropy Analysis and its Applications. Makino-Shoten, Tokyo (in Japanese).  
 Albert, R., 2006. Scale-free networks in cell biology. *J. Cell Sci.* 118, 4947–4957.  
 Albert, R., Barabási, A.-L., 2000. Dynamics of complex systems: scaling laws for the period of boolean networks. *Phys. Rev. Lett.* 84, 5660.  
 Albert, R., Barabási, A.-L., 2002. Statistical mechanics of complex networks. *Rev. Mod. Phys.* 74, 47–97 and references therein.  
 Aldana, M., 2003. Boolean dynamics of networks with scale-free topology. *Physica D* 185, 45–66.  
 Aldana, M., Cluzel, P., 2003. A natural class of robust networks. *Proc. Natl. Acad. Sci.* 100, 8710–8714.  
 Aldana, M., Coppersmith, S., Kadanoff, L.P., 2003. Boolean dynamics with random couplings. In: Kaplan, E., Marsden, J.E., Sreenivasan, K.R. (Eds.), *Perspectives and Problems in Nonlinear Science*. Springer, NY, pp. 23–90.  
 Aldana, M., Balleza, E., Kauffman, S., Resendiz, O., 2007. Robustness and evolvability in genetic regulatory networks. *J. Theor. Biol.* 245, 433–448.  
 Anderson, P.E., Jensen, H.J., 2005. Network properties, species abundance and evolution in a model of evolutionary ecology. *J. Theor. Biol.* 232, 551–558.  
 Andrade, R.F.S., Miranda, J.G.V., Lobao, T.P., 2006. Neighborhood properties of complex networks. *Phys. Rev. E* 73, 046101.  
 Bar-Yam, Y., Epstein, I.R., 2004. Response of complex networks to stimuli. *Proc. Natl. Acad. Sci.* 101, 4341–4345.  
 Barabási, A.-L., Oltvai, Z.N., 2004. Network biology: understanding the cell's functional organization. *Nat. Rev.* 5, 101–113.

Barabási, A.-L., Albert, R., Jeong, H., 1999. Mean-field theory for scale-free random networks. *Physica A* 272, 173–187.  
 Bastolla, U., Parisi, G., 1997. The critical line of Kauffman networks. *J. Theor. Biol.* 187, 117–133.  
 Bianconi, G., Marsili, M., 2006. Effect of degree correlations on the loop structure of scale-free networks. *Phys. Rev. E* 73, 066127.  
 Bianconi, G., Gulbahce, N., Motter, A.E., 2008. Local structure of directed networks. *Phys. Rev. Lett.* 100, 118701.  
 Bilke, S., Sjunnesson, F., 2001. Stability of the Kauffman model. *Phys. Rev. E* 65, 01629.  
 Billingsley, P., 1960. *Ergodic Theory and Information*. Wiley, New York.  
 Boccaletti, S., et al., 2006. Complex networks: structure and function. *Phys. Rep.* 424, 175.  
 Bornholdt, S., Sneppen, K., 2000. Robustness as an evolutionary principle. *Proc. R. Soc. London B* 267, 2281–2286.  
 Braunewell, S., Bornholdt, S., 2007. Superstability of the yeast cell-cycle dynamics: ensuring causality in the presence of biochemical stochasticity. *J. Theor. Biol.* 245, 638.  
 Castro e Silva, A., Kamphorst Leal da Silva, J., Mendes, J.F.F., 2004. A scale-free network with Boolean dynamics as a function of connectivity. *Phys. Rev. E* 70, 066140 cond-mat/0410469.  
 Ciliberti, S., Martin, O.C., Wagner, A., 2007. Robustness can evolve gradually in complex regulatory gene networks with varying topology. *PLoS Comput. Biol.* 3, 0164–0173.  
 Drossel, B., 2008. Random Boolean networks. In: H.G. Schuster (Ed.), *Reviews of Nonlinear Dynamics and Complexity*, vol. 1. Wiley, NY; arXiv:0706.3351v2.  
 Fox, J.J., Hill, C.C., 2001. From topology to dynamics in biochemical networks. *Chaos* 11, 809–815.  
 Fretter, C., Drossel, B., 2008. Response of Boolean networks to perturbations. *Eur. Phys. J. B* 62, 365–371.  
 Gardenes, J.G., Moreno, Y., Floria, L.M., 2006. Scale-free topologies and activatory–inhibitory interactions. *Chaos* 16, 015114.  
 Gecow, A., 2007. Emergence of growth, complexity threshold and structural tendencies during adaptive evolution of system. *EPNACS in ECCS'07 Dresden*, preprint.  
 Goh, K.-I., Kahng, B., Kim, D., 2001. Universal behavior of load distribution in scale-free networks. *Phys. Rev. Lett.* 87, 278701–1–4.  
 Greil, F., Drossel, B., 2007. Kauffman networks with threshold functions. *Eur. Phys. J. B* 57, 109–113.  
 Handrey, C., Ferraz, A., Herrmann, H.J., 2007. The Kauffman model on small-world topology. *Physica A* 373, 770–776.  
 Haydon, D.T., 2000. Maximally stable model ecosystems can be highly connected. *Ecology* 81, 2631–2636.  
 Holme, P., Ghoshal, G., 2006. Dynamics of networking agents competing for high centrality and low degree. *Phys. Rev. Lett.* 96, 098701.  
 Iguchi, K., Kinoshita, S., Yamada, H.S., 2005. Rugged fitness landscapes of Kauffman models with a scale-free network. *Phys. Rev. E* 72, 061901.  
 Iguchi, K., Kinoshita, S., Yamada, H.S., 2007. Boolean dynamics of Kauffman model with a scale-free network. *J. Theor. Biol.* 247, 138–151.  
 Jansen, V.A.A., Kokkoris, G.D., 2003. Complexity and stability revisited. *Ecol. Lett.* 6, 498–502.  
 Justa, W., Shmulevich, I., Konvalinac, J., 2004. The number and probability of canalizing functions. *Physica D* 197, 211–221.  
 Kauffman, S.A., 1969. Metabolic stability and epigenesis in randomly constructed genetic nets. *J. Theor. Biol.* 22, 437–467.  
 Kauffman, S.A., 1993. *Origins of Order: Self-Organization and Selection in Evolution*. Oxford University Press, Oxford.  
 Kauffman, S.A., 2003. Complexity and genetic networks. *Existence Project News* 2003.  
 Kauffman, S.A., 2004a. The ensemble approach to understand genetic regulatory networks. *Physica A* 340, 733–740.  
 Kauffman, S.A., 2004b. A proposal for using the ensemble approach to understand genetic regulatory networks. *J. Theor. Biol.* 230, 581–590.  
 Kauffman, S.A., Peterson, C., Samelson, B., Troein, C., 2003. Random Boolean network models and the yeast transcriptional network. *Proc. Natl. Acad. Sci. USA* 100, 14796–14799.  
 Kinoshita, S., Iguchi, K., Yamada, H.S., 2008a. Attractor states of Boolean dynamics in complex networks. *AIP Conf. Proc.* 982, 768–771.  
 Kinoshita, S., Iguchi, K., Yamada, H.S., 2008b. *Prog. Theor. Phys. Suppl.* 173, 342–350.  
 Kinoshita, S., Iguchi, K., Yamada, H.S., 2008c. in preparation.  
 Klemm, K., Bornholdt, S., 2005. Topology of biological networks and reliability of information processing. *Proc. Natl. Acad. Sci.* 102, 18414–18419.  
 Kohane, I.S., Kho, A.T., Butte, A.J., 2002. *Microarrays for an Integrative Genomics*. MIT Press, NY.  
 Kondoh, M., 2003. Foraging adaptation and the relationship between food-web complexity and stability. *Science* 299, 1388–1391.  
 Krawitz, P., Shmulevich, I., 2007a. Basin entropy in Boolean network ensembles. *Phys. Rev. Lett.* 98, 158701.  
 Krawitz, P., Shmulevich, I., 2007b. Basin entropy in Boolean network ensembles. *Phys. Rev. Lett.* 98, 036115.  
 Lee, T.I., et al., 2002. Transcriptional regulatory networks in *Saccharomyces cerevisiae*. *Science* 298, 799–804.  
 Levin, S.A., 2000. *Fragile Dominion: Complexity and the Commons*. Perseus Publishing, Cambridge.  
 Li, F., et al., 2004. The yeast cell-cycle network is robustly designed. *Proc. Natl. Acad. Sci.* 101, 4781.

- Liu, M., Bassler, K.E., 2006. Emergent criticality from co-evolution in random Boolean networks. *Phys. Rev. E* 74, 041910 cond-mat/0605020.
- May, R., 1999. Unanswered questions in ecology. *Philos. Trans. R. Soc. London B* 354, 1951–1959.
- Maynard Smith, J., Szathmary, E., 1995. *The Major Transitions in Evolution*. Spektrum Akademischer Verlag.
- Maynard Smith, J., Szathmary, E., 1999. *The Origins of Life: From the Birth of Life to the Origin of Language*. Oxford University Press, Oxford.
- Monte, J.M., Liu, M.M., Sheya, A.A., Kitami, T., 2005. Definitions, measures, and models of robustness in gene regulatory networks. Report of Research Work for CSS05, July 2005.
- Mount, D.W., 2004. *Bioinformatics: Sequence and Genome Analysis*, second ed. Cold Spring Harbor Laboratory Press.
- Newman, M.E.J., 2002. Assortative mixing in networks. *Phys. Rev. Lett.* 89, 208701.
- Nykter, M., et al., 2008. Critical networks exhibit maximal information diversity in structure-dynamics relationships. *Phys. Rev. Lett.* 100, 058702.
- Oikonomou, P., Cluzel, P., 2006. Effects of topology on network evolution. *Nature Physics* 2, 532–536.
- Oosawa, C., Savageau, A., 2002. Effects of alternative connectivity on behavior of randomly constructed Boolean networks. *Physica D* 170, 143–161.
- Paczuski, M., Bassler, K.E., Corral, A., 2000. Self-organized networks of competing Boolean agents. *Phys. Rev. Lett.* 84, 3185–3188.
- Rohlf, T., Gulbahce, N., Teuscher, C., 2007. Damage spreading and criticality in finite random dynamical networks. *Phys. Rev. Lett.* 99, 248701.
- Sawhill, B.K., Kauffman, S.A., 1997. Phase transitions in logic networks. Working paper, Sana Fe Institute.
- Sen, P., et al., 2003. Small-world properties of the Indian railway network. *Phys. Rev. E* 67, 036106.
- Serra, R., Villani, M., Agostini, L., 2003. On the dynamics of scale-free Boolean networks. WIRN VIETRI 2003. *Lecture Notes in Computer Science*, vol. 2859, Springer, Berlin, pp. 43–49.
- Shen-Orr, S.S., et al., 2002. Network motifs in the transcriptional regulation network of *Escherichia coli*. *Nature Genetics* 31, 64–68.
- Skarja, M., Remic, B., Jerman, I., 2004. Boolean networks with variable number of inputs (K). *Chaos* 14, 205–216.
- Socolar, J.E.S., Kauffman, S.A., 2003. Scaling in ordered and critical random Boolean networks. *Phys. Rev. Lett.* 90, 068702.
- Szejka, A., Drossel, B., 2007. Evolution of canalizing Boolean networks. *Eur. Phys. J. B* 56, 373–380.
- Ueda, H.R., et al., 2004. Universality and flexibility in gene expression from bacteria to human. *Proc. Natl. Acad. Sci.* 101, 3765–3769.
- Wagner, A., 2005. *Robustness and Evolvability in Living Systems*. Princeton University Press, NY.
- Wang, S.-J., Wu, A.-C., Wu, Z.-X., Xu, X.-J., Wang, Y.-H., 2007. Response of degree-correlated scale-free networks to stimuli. *Phys. Rev. E* 75, 046113 arXiv:0704.1849v1 [cond-mat.dis-nn].
- Wang, X.F., Chen, G.-R., 2002. Synchronization in scale-free dynamical networks: robustness and fragility. *IEEE Trans. Circuits Sys.* 49, 54–61.
- Watts, D.J., Strogatz, S.H., 1998. Collective dynamics of 'small-world' networks. *Nature* 393, 440–442.
- White, D.R., Kejzar, N., Tsallis, C., Farmer, D., White, S., 2006. A generative model for feedback networks. *Phys. Rev. E* 73, 016119-1-8 cond-mat/0508028.
- Zhang, S.Q., Hayashida, M., Akutsu, T., Ching, W.-K., Ng, M.K., 2007. *EURASIP J. Bioinform. Syst. Biol.* 2007, 20180.